

# Theory and Practice of Free-Electron Lasers

## Particle Accelerator School Day 4

Dinh Nguyen, Steven Russell  
& Nathan Moody  
Los Alamos National Laboratory

# Course Content

- Chapter 1. Introduction to Free-Electron Lasers
  - Chapter 2. Basics of Relativistic Dynamics
  - Chapter 3. One-dimensional Theory of FEL
  - Chapter 4. Optical Architectures
  - Chapter 5. Wigglers
  - Chapter 6. RF Linear Accelerators
  - Chapter 7. Electron Injectors
- Day 1
- Day 2
- Day 3
- Day 4

# Chapter 6

## RF Linear Accelerators (continued)

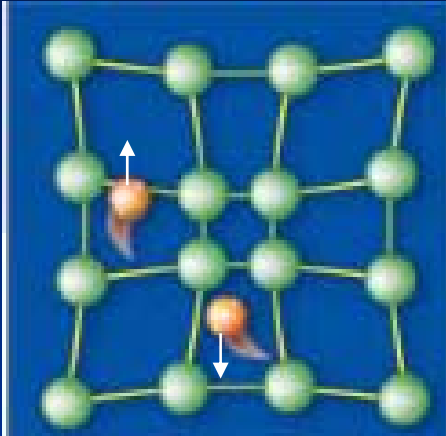
# RF Linear Accelerators (Linac)

- Introduction to RF Linac
- Properties of RF Cavities
- Coupled Cavity Linac
- Superconducting RF Linac
- Energy Recovery Linac

# Superconducting RF Linacs

- RF Superconductivity
  - Meissner effect
  - Surface resistance
  - Temperature dependence
- Superconducting cavities
  - Cavity designs
  - Cavity Q versus  $E_{\text{acc}}$

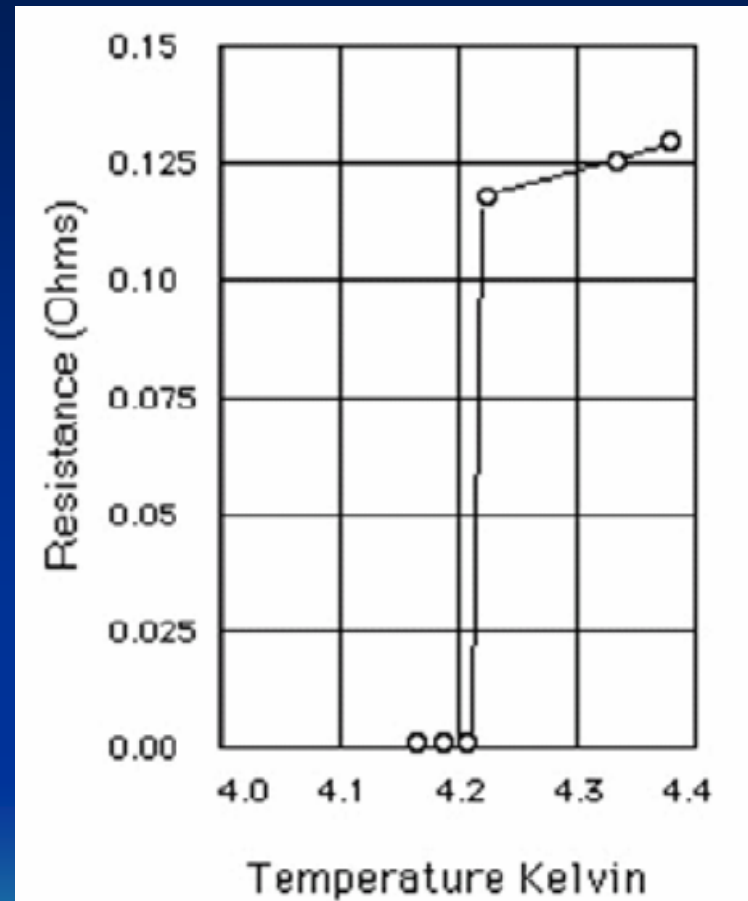
# Superconductivity



**Coopers pair:** Two electrons with anti-parallel momenta and spins attracting each other via exchange of lattice phonons.

**Bose condensation:** Overlapping Coopers pairs condensing into a coherent superconducting state at low temperature.

**Critical temperature,  $T_c$ :** Temperature below which Coopers pairs form with binding energy  $\sim 10^{-4} - 10^{-3}$  eV.



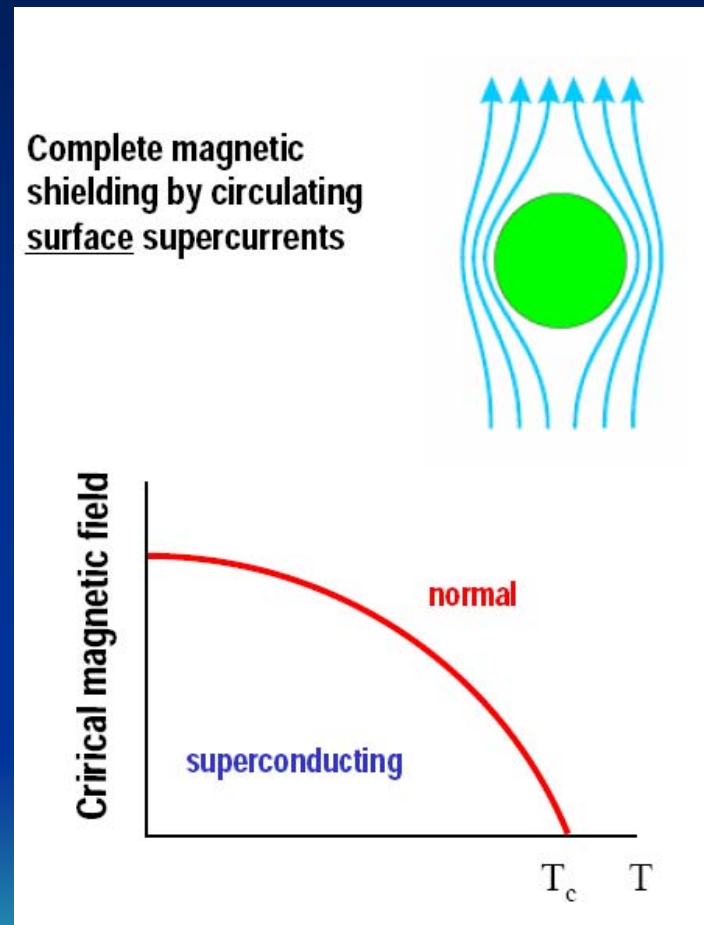
Discovery of superconductivity by Kamerlingh-Onnes and Holst in 1911  
Courtesy of A. Gurevich

# Meissner Effect and Critical Field

- Magnetic field is expelled from a superconductor at  $T < T_c$
- Superconductivity is destroyed at  $H > H_c$  (critical magnetic field)
- Empirical formula for  $H_c$

$$H_c = H_{c2}(0) \left( 1 - \left( \frac{T}{T_c} \right)^2 \right)$$

- For Nb (type II superconductor)
  - $T_c$  is 9.2K
  - $\mu_0 H_{c2}(0)$  is 0.24 T
  - At 2K,  $\mu_0 H_c$  is 0.22 T



Courtesy of A. Gurevich

# Surface Resistance of Niobium

Niobium surface resistance at low temperature has two components: BCS (Bardeen-Cooper-Schrieffer) resistance and residual resistance

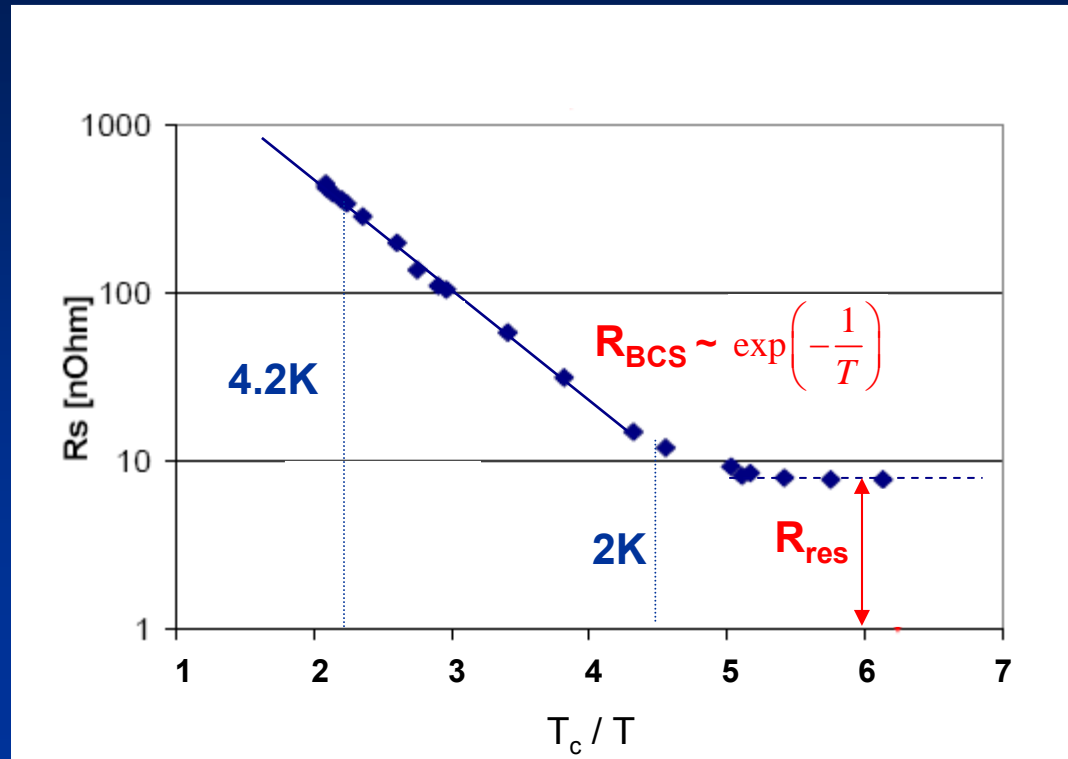
$$R_s \approx 2 \times 10^{-4} \Omega \left( \frac{f}{1.5 \text{GHz}} \right)^2 \frac{1}{T} \exp\left( \frac{-17.67}{T} \right) + R_{\text{residual}}$$

BCS resistance scales with  $f^2$ . SRF accelerators have lower BCS resistance (loss) at low frequency. To minimize BCS resistance, SRF cavities with  $f > 500$  MHz have to be cooled to 2K.

Residual resistance depends on material purity and trapped magnetic field. The earth magnetic field has to be shielded with mu metal around the cavities.

- High-purity niobium sheet metals have low residual resistance (1 – 10 nΩ)
- Residual resistance =  $3.75 \text{ n}\Omega/\mu\text{T} (f / \text{GHz})^{0.5}$  so trapped magnetic field (trapped flux) should be avoided to minimize residual resistance.

# Surface Resistance vs. 1/T



Geometric factor  $G (= Q_0 R_S)$  is about  $270 \Omega$

Nb at 4.2K at 1.3 GHz

$R_{BCS} > 500 \text{ n}\Omega$

$R_S > 500 \text{ n}\Omega$

$Q_0 < 5 \times 10^8$

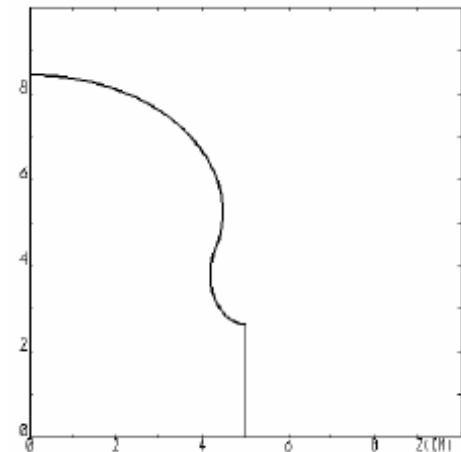
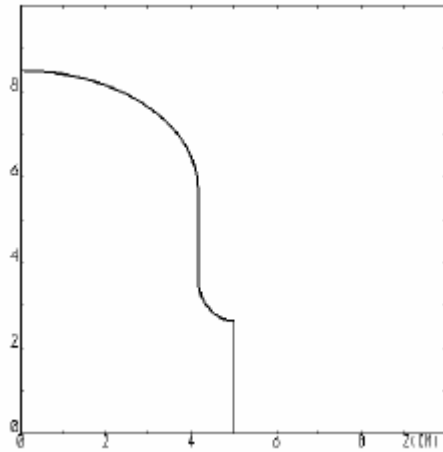
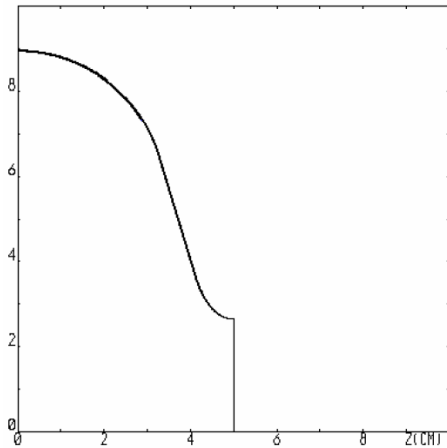
Nb at 2K at 1.3 GHz

$R_{BCS} = 7 \text{ n}\Omega$

$R_S = 15 \text{ n}\Omega$

$Q_0 = 2 \times 10^{10}$

# Elliptical Cavity Designs



Optimized TESLA

Optimized low-loss

Optimized re-entrant

$TM_{010}$

$G^*R/Q$  30840  $\Omega^2$

37970  $\Omega^2$

38380  $\Omega^2$

$E_p / E_a$  1.98

2.36

2.3

$B_p / E_a$  4.15 mT/(MV/m)

3.61 mT/(MV/m)

3.57 mT/(MV/m)

$k_{CC}$  1.9

1.52

1.56

*HOM*

$k_{\perp}$  0.23

0.38

0.38

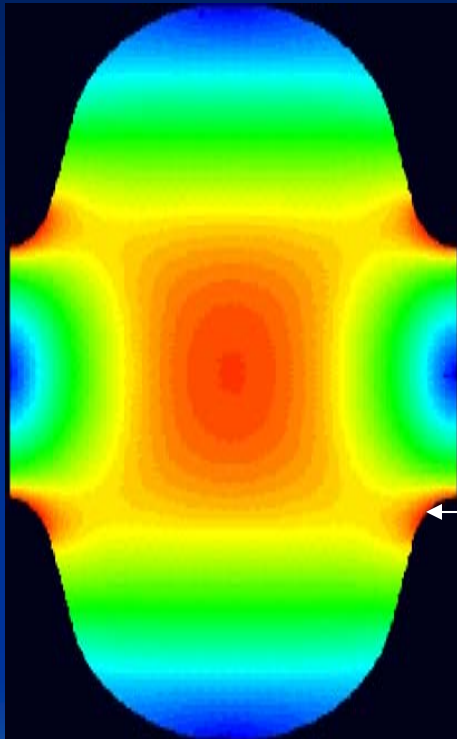
$k_{\parallel}$  1.46

1.72

1.75

# Peak Fields to Average Gradient

Peak electric field



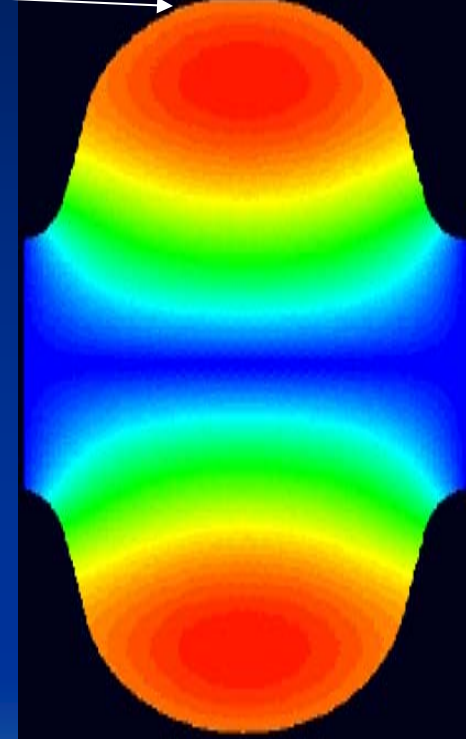
Highest  $E_p$   
 $E_p/E_a \sim 2$

High electric fields cause field emission → Q degradation

Highest  $B_p$

$$B_p/E_a \sim 4 \text{ mT}/(\text{MV}/\text{m})$$

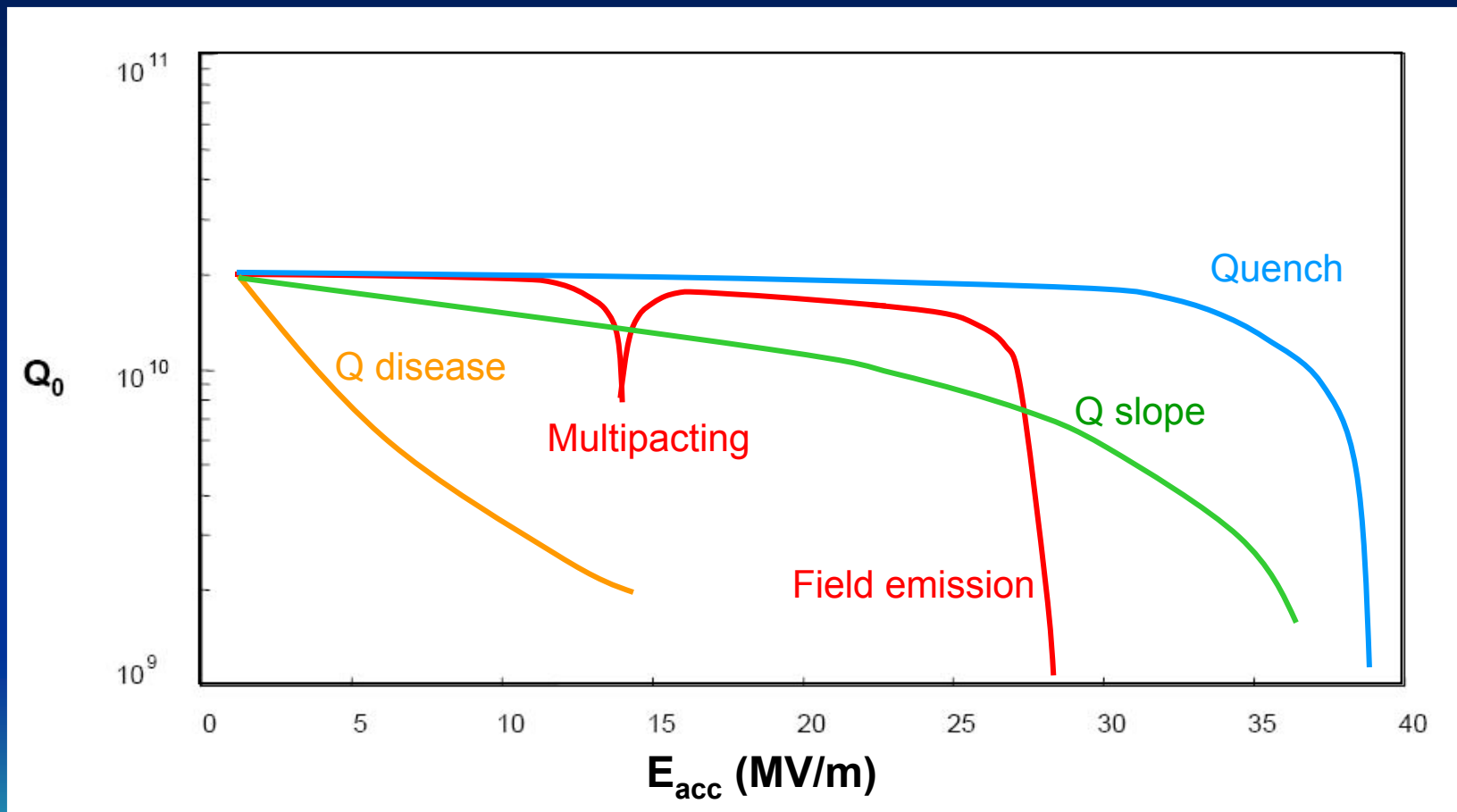
Peak magnetic field



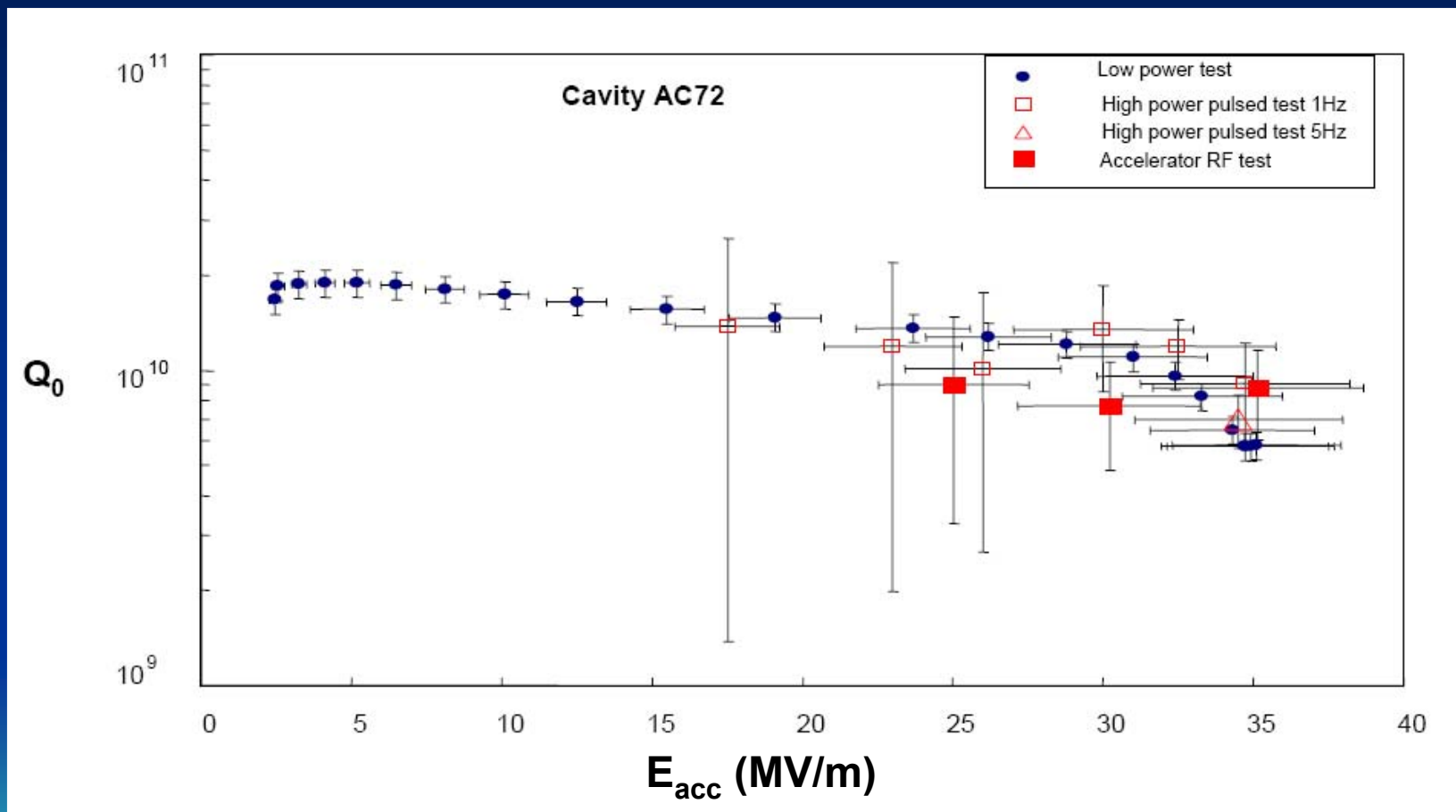
High magnetic fields cause RF heating → quench

Courtesy of J. Sekutowics

# Cavity Q vs. Gradient



# Unloaded Q vs Gradient of a TESLA 1.3 GHz SRF Cavity



Courtesy of D. Reschke

# Energy Recovery Linac (ERL)

- Energy Recovery Linac
  - Benefits and Risks
  - Same Cavity versus Different Cavity
  - Voltage Phase Diagram
- Instabilities
  - RF Instabilities
  - Beam Break-up Instabilities
- HOM Damping

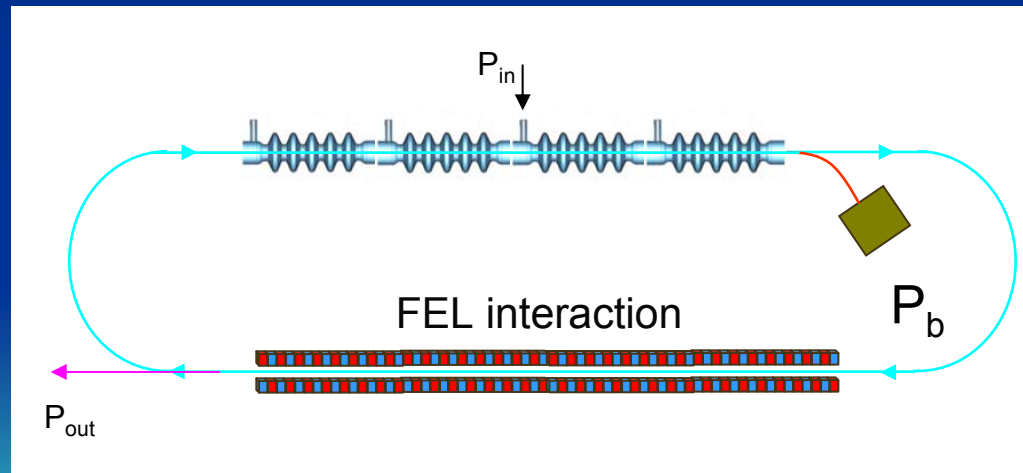
# Benefits and Risks of ERL

## *Benefits*

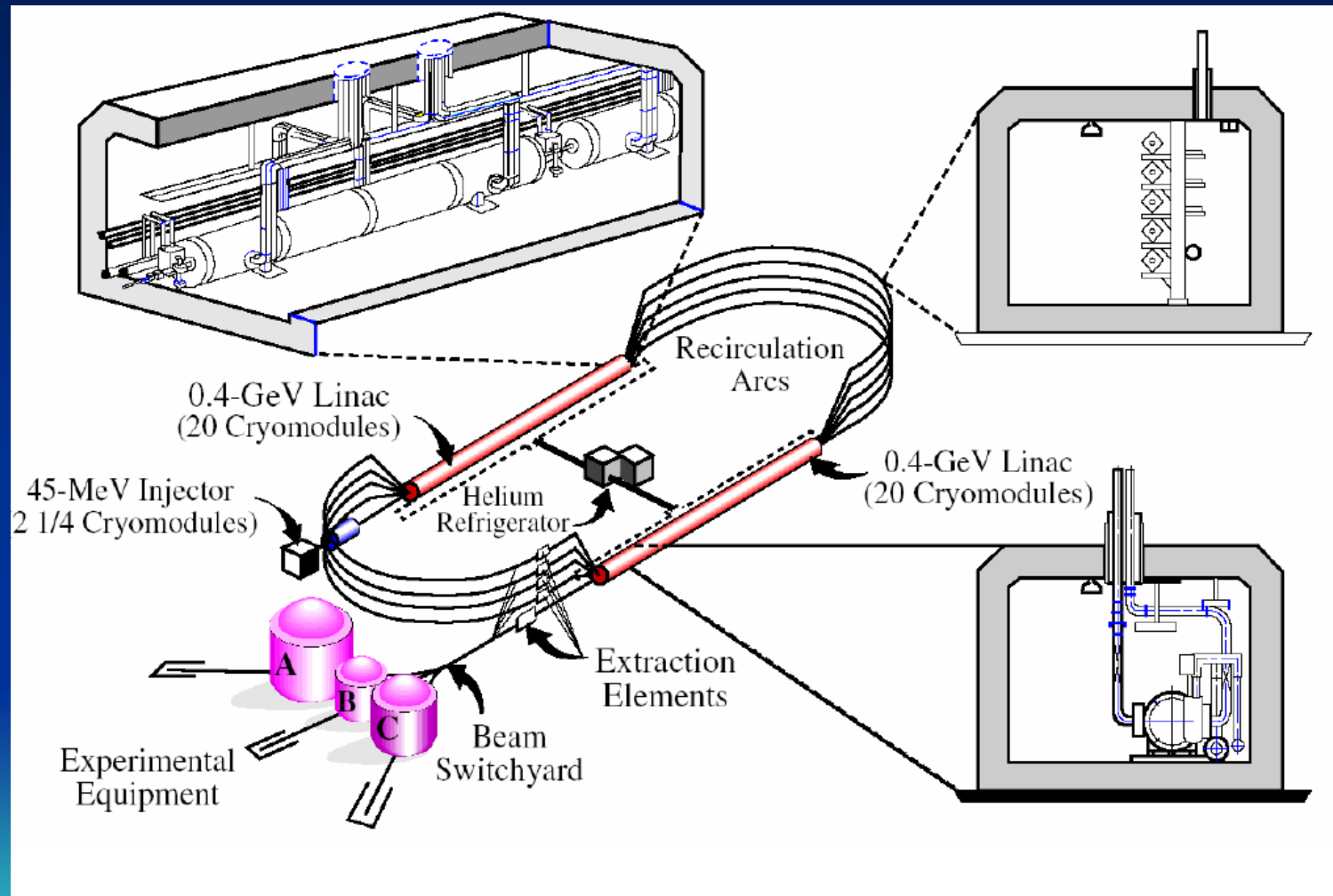
- Reduce RF power consumption (Increase wall-plug efficiency)
- Achieve much higher electron beam power than input RF power

## *Risks*

- Susceptible to instabilities
  - RF instabilities
  - Beam break-up instabilities
- Difficult to recover energy due to large energy spread in spent beams

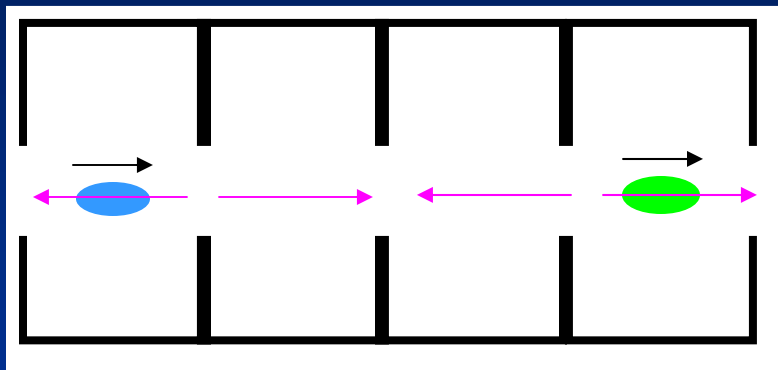


# Example of ERL: CEBAF

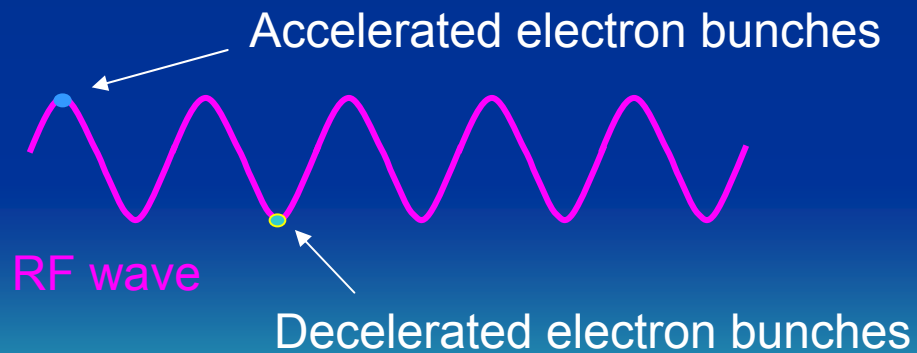
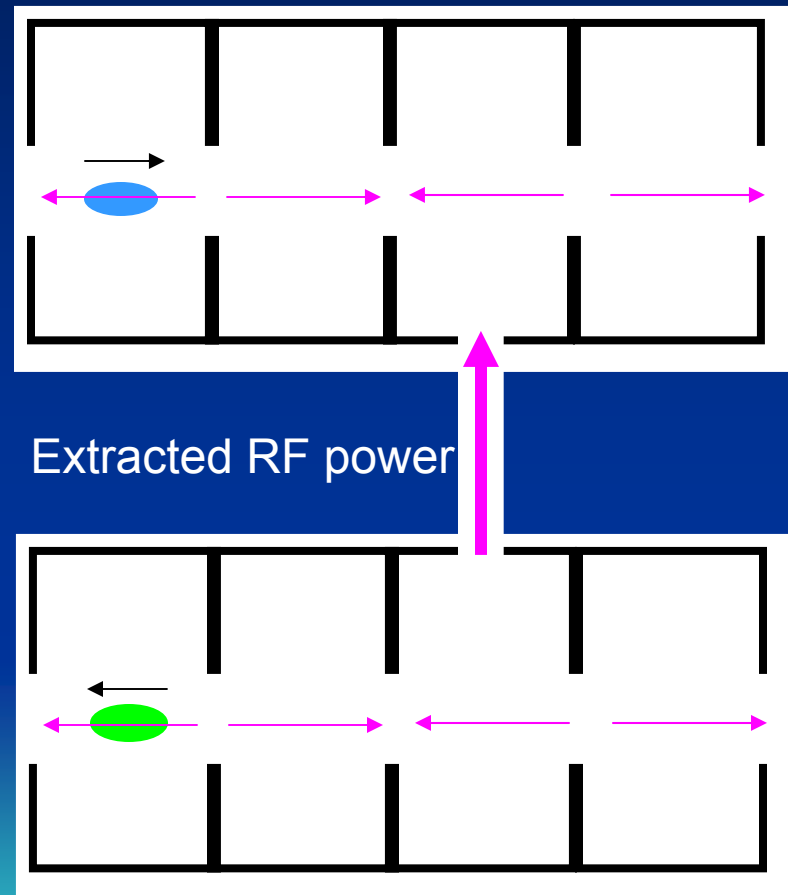


# Same Cavity vs Different Cavity

Same cavity energy recovery



Different cavity energy recovery



# RF Instabilities

- Interaction between cavity power and beam

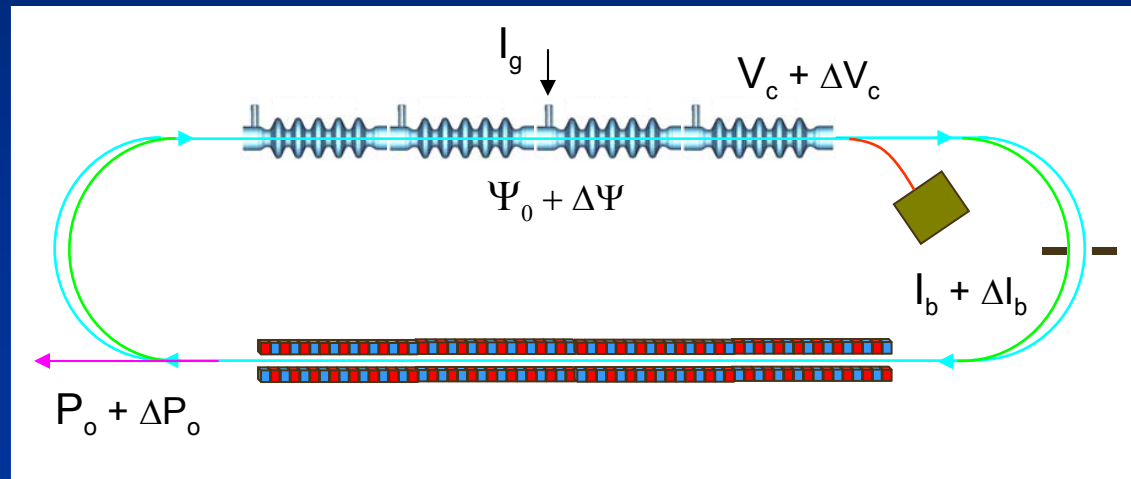
$$\frac{d\tilde{V}_c}{dt} + \frac{\omega_0}{2Q_L}(1 - i \tan \Psi)\tilde{V}_c = \frac{\omega_0 R}{2Q_L}(\tilde{I}_g - \tilde{I}_b)$$

- Fluctuations in cavity field cause

Beam loss

Phase errors

FEL power fluctuations

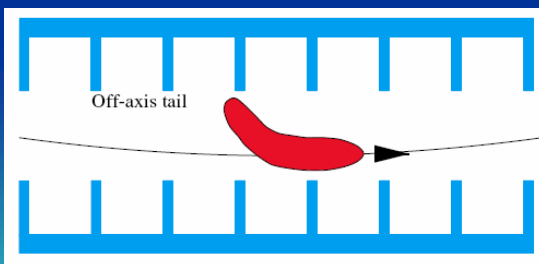


- All three of the above can increase beam energy fluctuations, resulting in additional beam loss, phase errors or FEL fluctuations, hence instabilities.

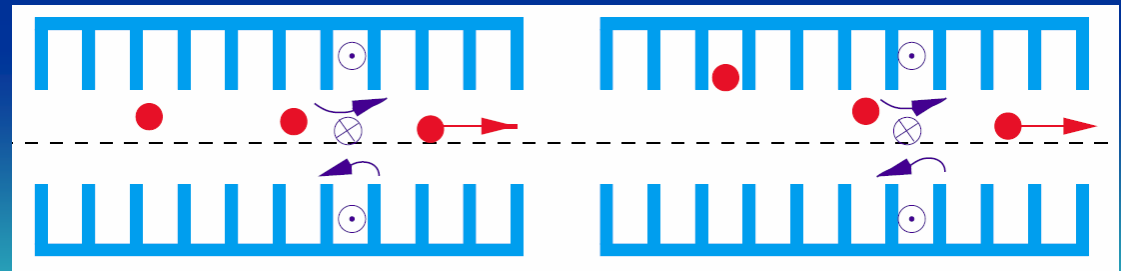
# Beam Break-up Instabilities (BBU)

- An electron traversing an accelerating cavity off axis will excite higher order modes (HOM), some of which are dipole modes, of the cavity
- The coupling between the beam and the dipole mode is proportional to the beam current and the transverse position offset
- The dipole modes could deflect a following particle to a larger amplitude, thereby increasing the coupling to and the strength of the dipole modes which would deflect following bunches further.

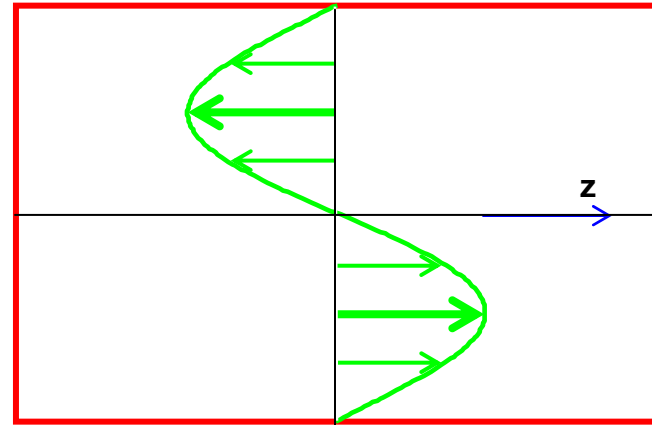
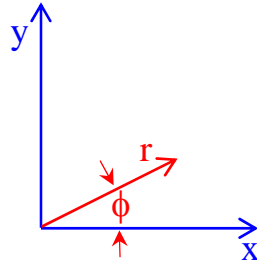
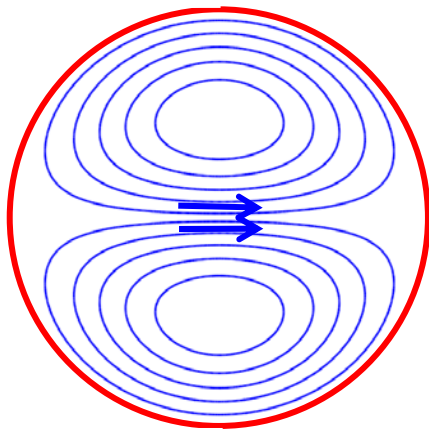
Single-bunch BBU  
(head to tail kick)



Multi-bunch BBU  
(deflection and beam loss)



# Higher Order Modes (HOM)



$$B_r = -B_0 \frac{J_1(kr)}{kr} \cos(\phi) \sin(\omega t)$$

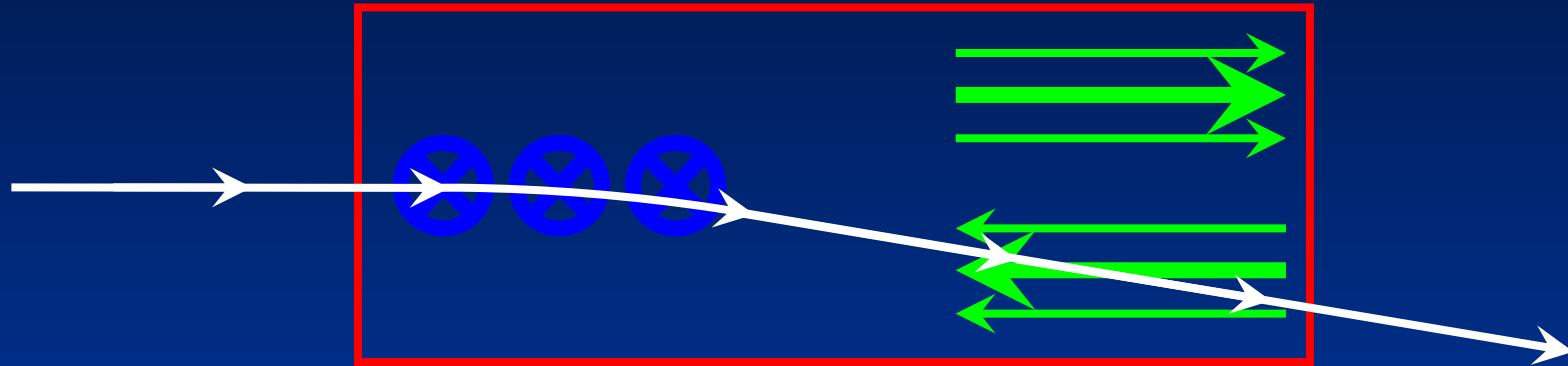
$$B_\phi = B_0 J_1'(kr) \sin(\phi) \sin(\omega t)$$

$$E_z = B_0 c J_1(kr) \sin(\phi) \cos(\omega t)$$

$$k = \frac{\omega}{c} = \frac{2\pi}{\lambda} = \frac{3.833}{a}$$

Recall the fundamental  $k = 2.405/a \rightarrow f_{\text{dipole}} \sim 1.5 f_{\text{fundamental}}$

# Single-pass Regenerative BBU



The on-axis magnetic field of the  $TM_{011}$  mode can impart transverse momentum to an electron. By the end of the cavity the beam is off-axis and can exchange energy with the axial electric field. The power of  $TM_{011}$  mode grows.

$$f_{\text{fundamental}} = 1.5 \text{ GHz}$$

$$f_d \approx 1.5 f_{\text{fundamental}} \approx 2 \text{ GHz}$$

$$\lambda_d = 15 \text{ cm}$$

$$V_{\text{beam}} = 10 \text{ MV}$$

$$R_d/Q = 100 \Omega$$

$$Q_L = 10^5$$

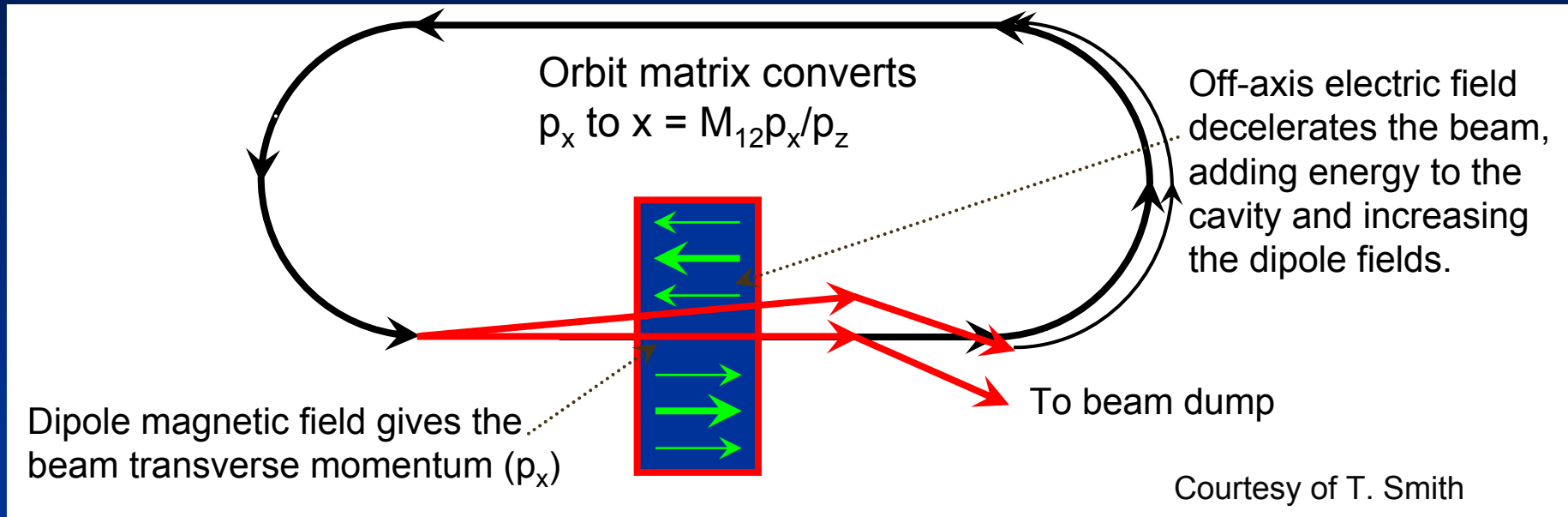
$$I_{\text{threshold}} \approx 240 \text{ mA}$$

Threshold current for single-pass BBU

$$I_{\text{threshold}} \approx \left( \frac{\pi}{2} \right) \frac{\lambda_d V_{\text{beam}}}{(R_d/Q) Q_L}$$

Courtesy of T. Smith

# Regenerative Two-pass BBU



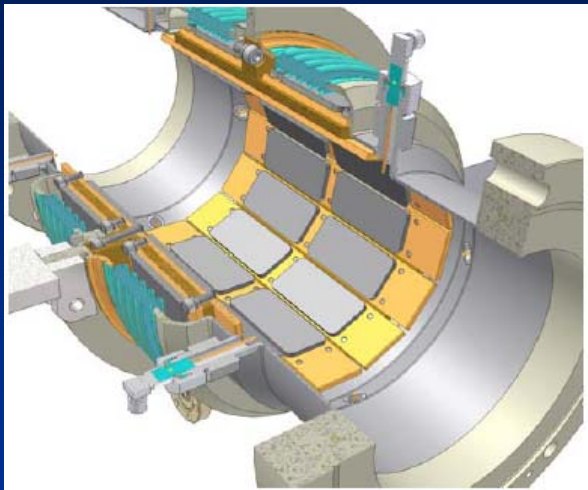
Threshold current for two-pass BBU

$$I_{threshold} \approx \frac{-\lambda_d V_{beam}}{\pi(R_d/Q)Q_L M_{12} \sin(\omega_d T_r)}$$

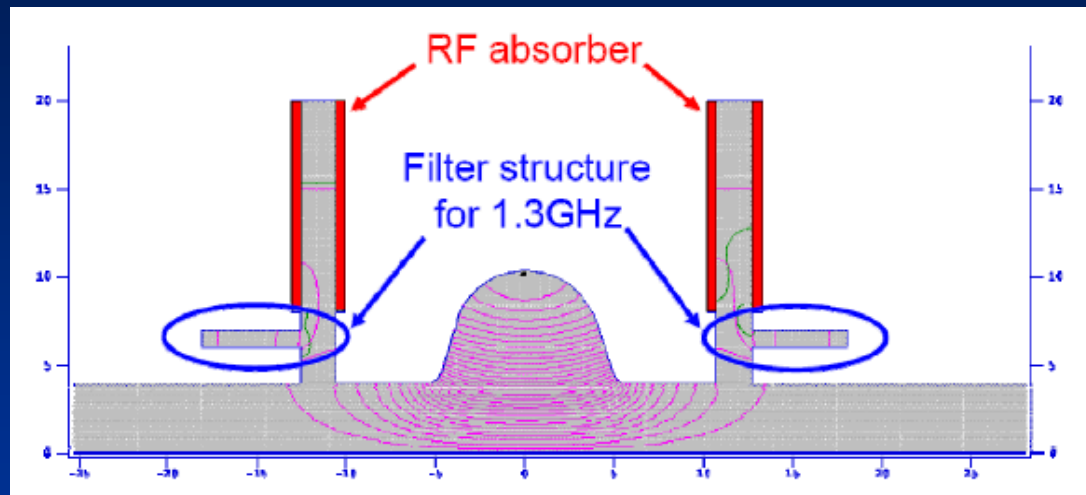
$$R_d = r_d L_{cavity}$$

With the same cavity as before, and assuming  $M_{12} = 1$  meter, the BBU threshold is now only **12 mA**, 20 times lower than the single-pass BBU

# HOM Damping



Ferrite absorber tiles



Single-cell SRF cavity with HOM couplers

Threshold current for two-pass BBU

$$I_{threshold} \approx \frac{-\lambda_d V_{beam}}{\pi(R_d/Q)Q_L M_{12} \sin(\omega_d T_r)}$$

Design a cavity with low R/Q ratios for the HOM. Then, couple the HOM into absorbers to reduce their loaded Q, thereby increasing the BBU threshold.

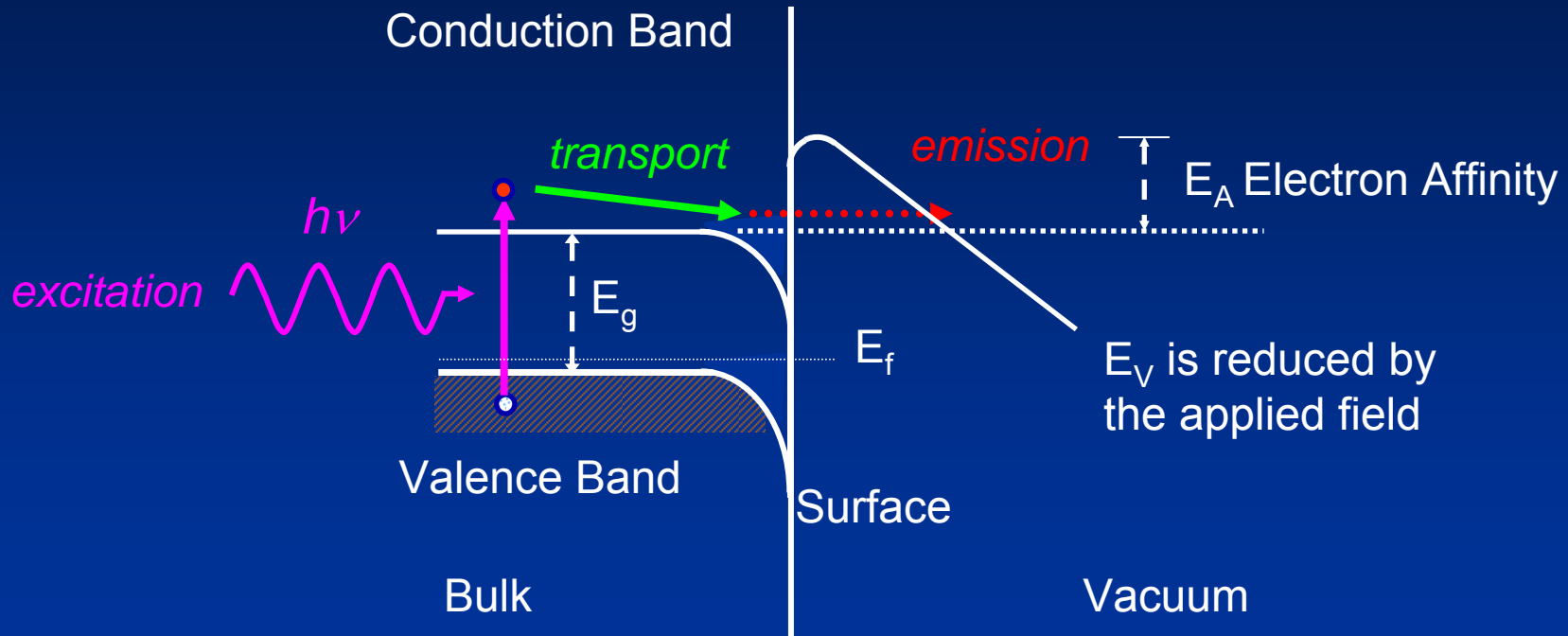
# Chapter 7

## Electron Injectors

# Typical Injector Performance

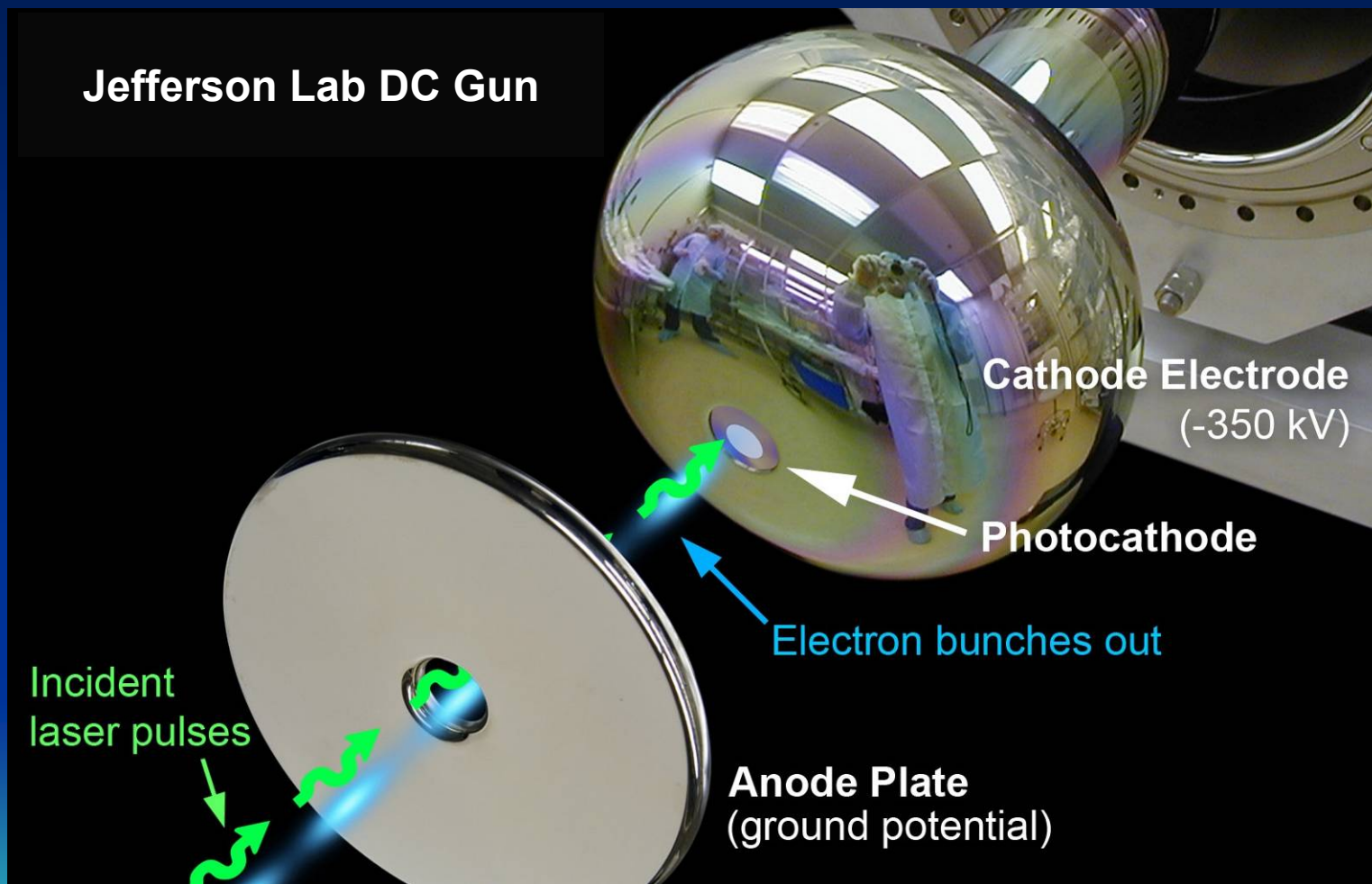
	DC Gun	Pulsed NCRF	High-duty NCRF	SRF Injector
Gradient (MV/m)	6	100	26	13.5
Energy (keV)	350	5000	2000	2100
Bunch charge (pC)	135	1000	7000	200
Average current (mA)	10	<0.001	32	<1
Transverse emittance (mm-mrad or $\mu\text{m}$ )	10	1.2	10	3
Bunch length (ps)	50	5	20	15
Photocathodes	GaAs	Cu	$\text{K}_2\text{CsSb}$	$\text{Cs}_2\text{Te}$
Photon energy (eV)	2.3	4.6	2.3	4.6
Photon wavelength (nm)	530	266	530	266
Photocathode lifetime	days	months	hours	months

# Photo-emission in a Semiconductor Photocathode



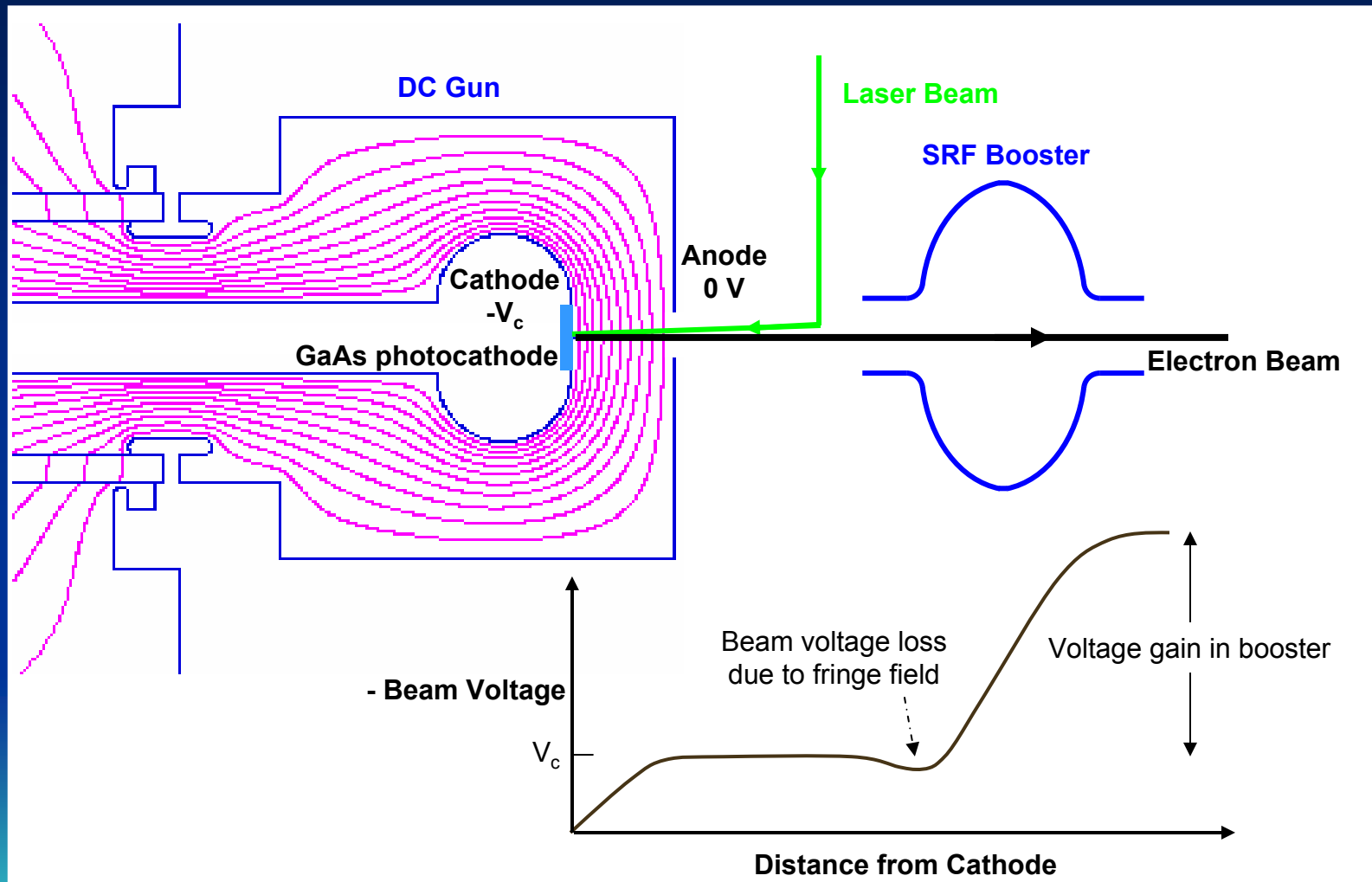
Electrons are excited by the laser from the valence band to the conduction band. During their transport from the bulk to the surface, the electrons undergo electron-phonon collisions and lose energy. Photoemission occurs as a tunneling process through the potential barrier at the solid-vacuum interface. The barrier height is determined by the electron affinity and the barrier width is determined by the applied electric field.

# DC Injector



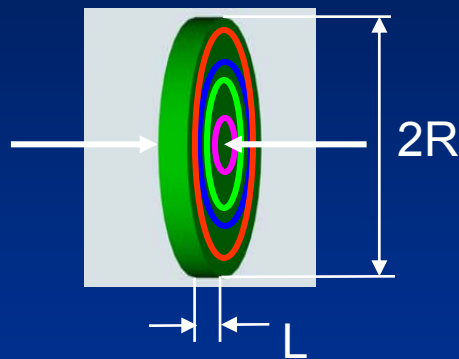
Courtesy of C. Hernandez-Garcia

# DC Injector and SRF Booster Cavity

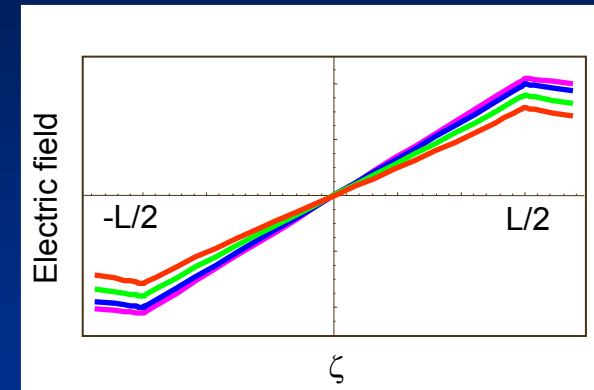


# Space Charge Effects

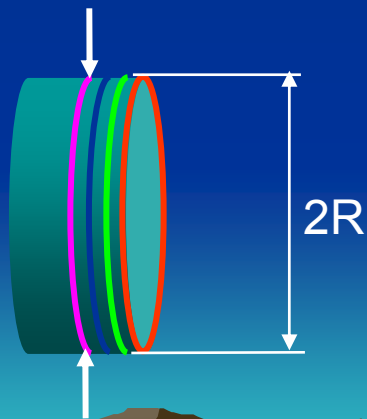
Longitudinal space charge field



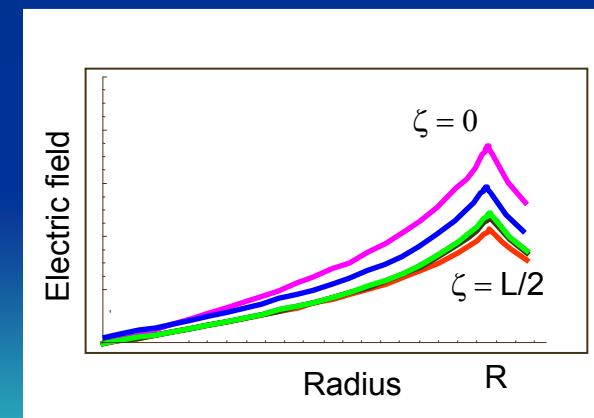
$$E_z(\zeta_0) = \frac{\int_{-L/2}^{\zeta_0} \rho(\zeta) d\zeta - \int_{\zeta_0}^{L/2} \rho(\zeta) d\zeta}{\epsilon_0 \pi r^2}$$



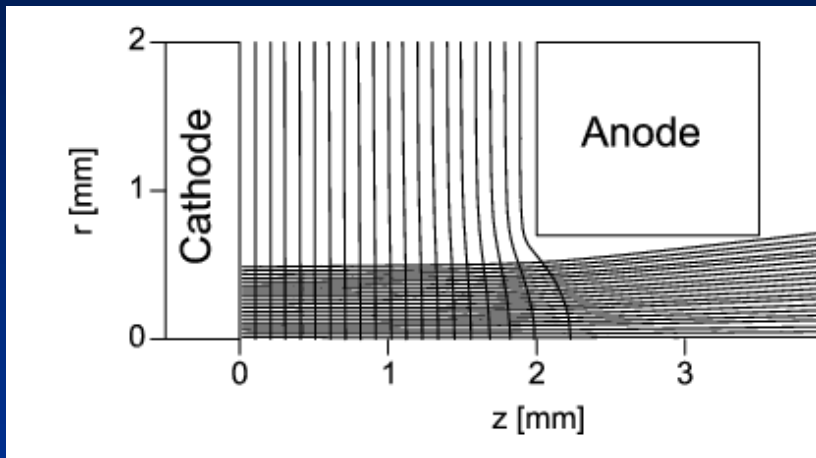
Radial space charge field



$$E_r(r_0) = \frac{\int_0^{r_0} \rho(r) dr}{\epsilon_0 \pi r_0^2}$$



# Beam Emittance with DC Guns

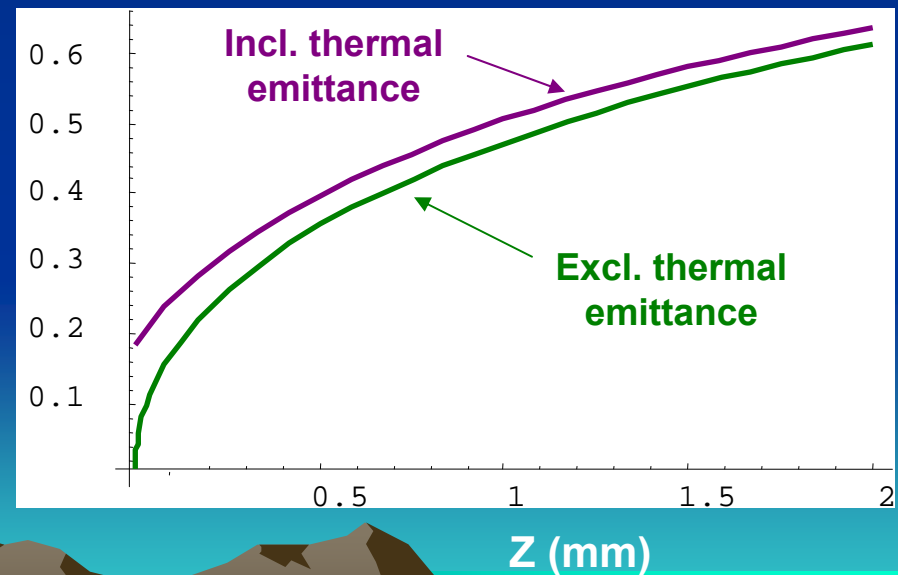
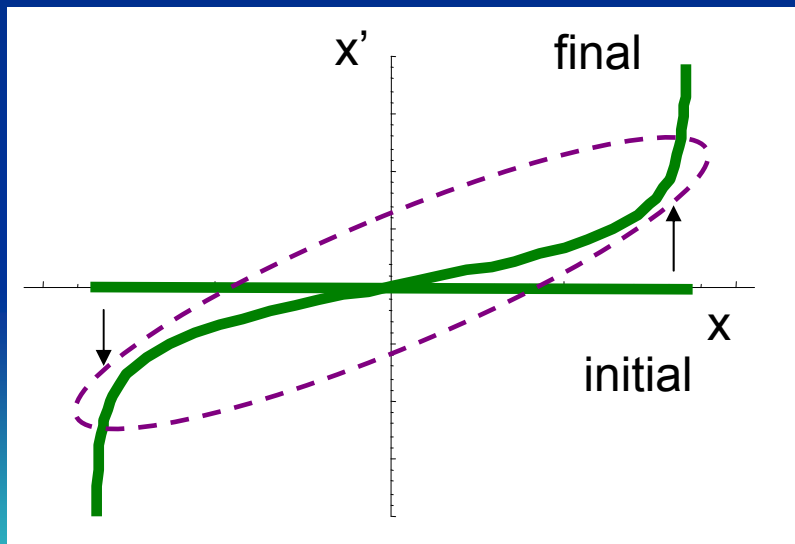


$$\varepsilon_{n,x} = 0.038 \frac{Q}{\varepsilon_0 E_0 \pi R} \log(\gamma + \sqrt{\gamma^2 - 1})$$

Bunch charge

Electric field

Emission radius



# Envelope Equation in Drift

Envelope equation for electron beams in a drift (no acceleration or focusing)

Peak current

Thermal emittance

$$\sigma'' - \frac{I}{\beta^3 \gamma^3 I_0 \sigma} - \frac{\varepsilon_T^2}{\beta^2 \gamma^2 \sigma^3} = 0$$

$\sigma'' = \frac{d^2 \sigma}{dz^2}$

$\beta = \frac{v}{c}$

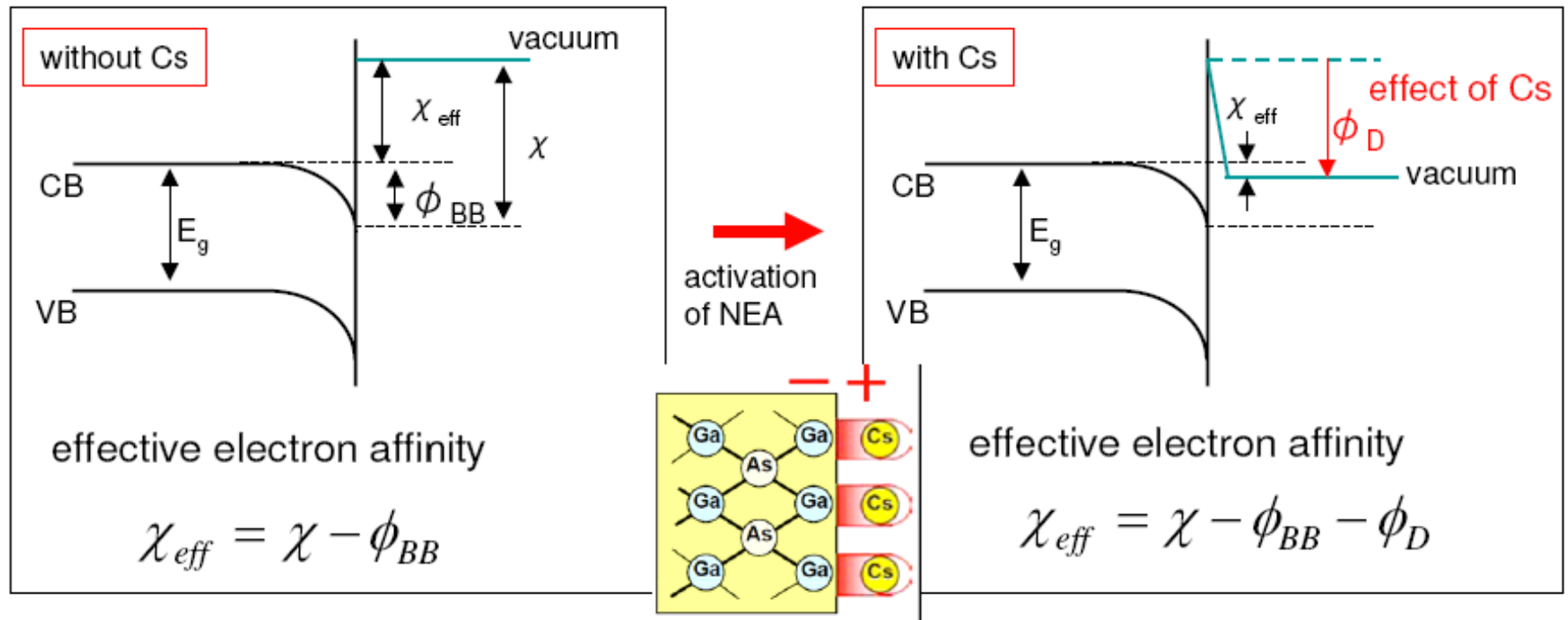
rms radius

Alfven current (17 kA)

$$\varepsilon_T = \sigma_0 \sqrt{\frac{kT}{mc^2}}$$

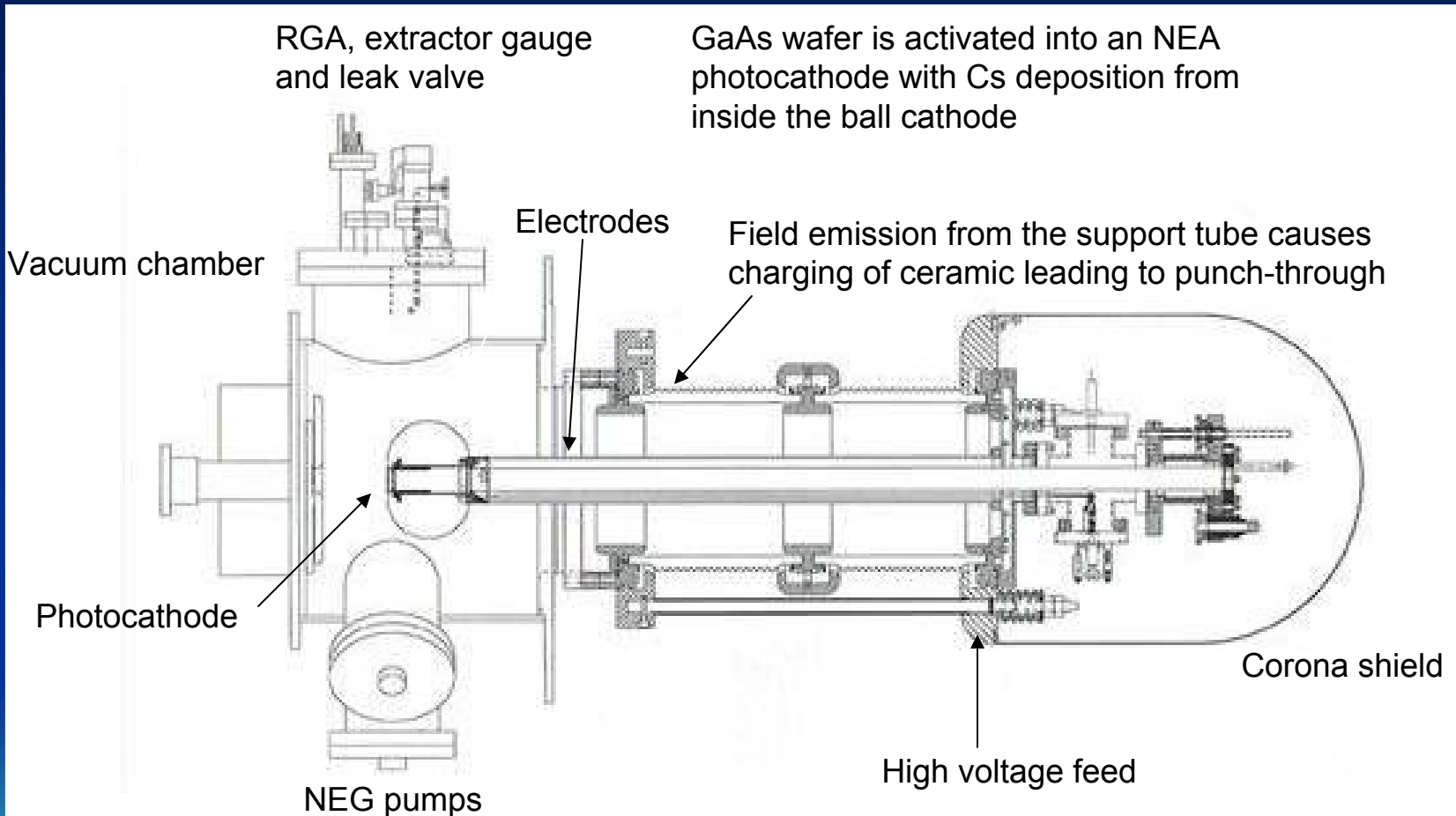
The beam envelope equation describes the forces acting on the beam envelope radius. The signs of both terms on the left hand side (other than the second derivative term) are negative, indicating the beam sees defocusing forces. The second term is the space-charge induced expansion. The third term is the thermal emittance expansion. Note the use of  $\beta$  because the low-energy beams are not quite relativistic in the drift.

# GaAs Photoemission



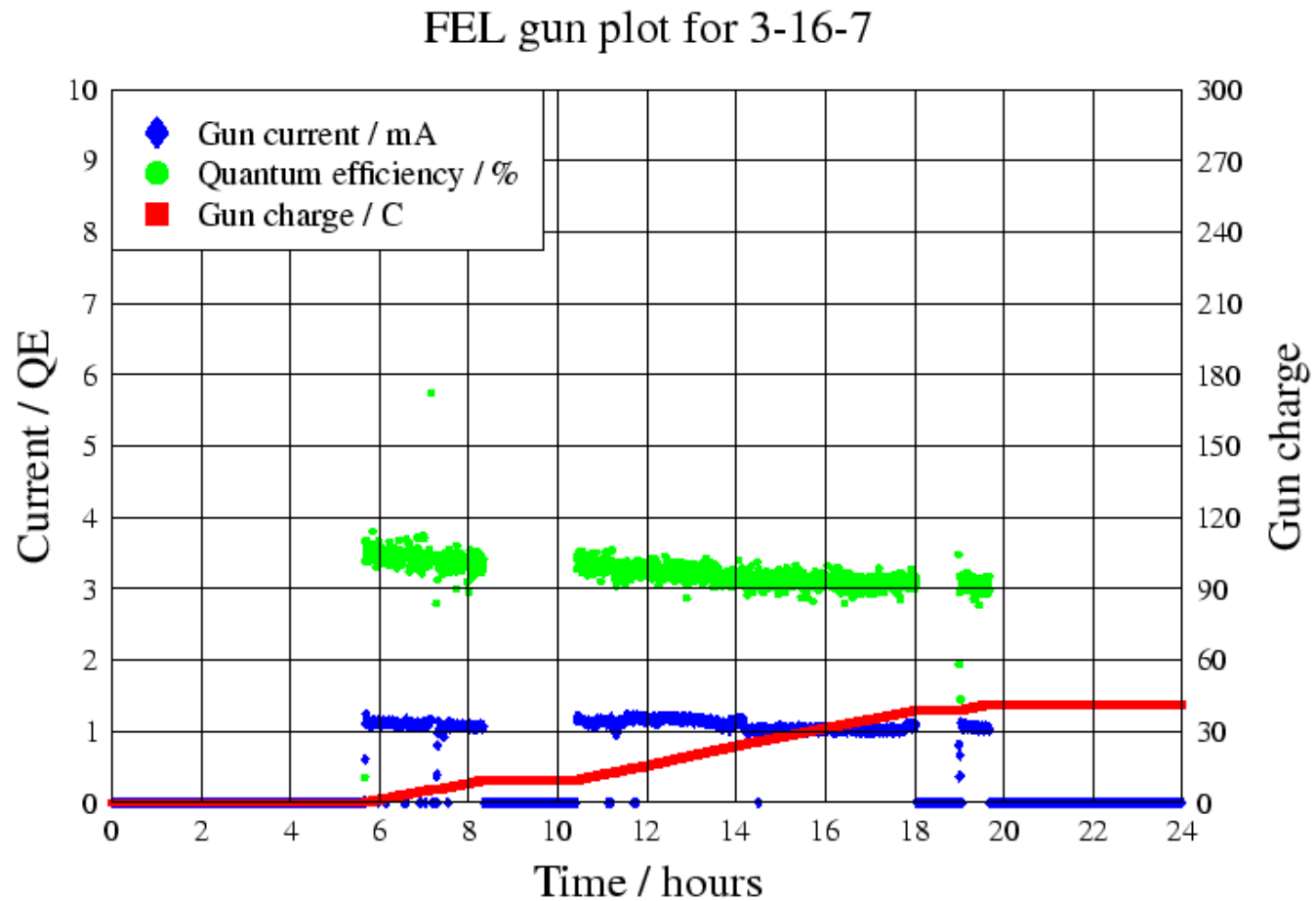
The quantum efficiency (QE) of GaAs cathode is enhanced by adding a monolayer of cesium to the surface. Cesium reduces the effective electron affinity by lowering the vacuum energy level to below the bulk energy level. Cesium GaAs is thus a negative electron affinity (NEA) photocathode.

# Schematics of the JLab DC Gun



Courtesy of C. Sinclair

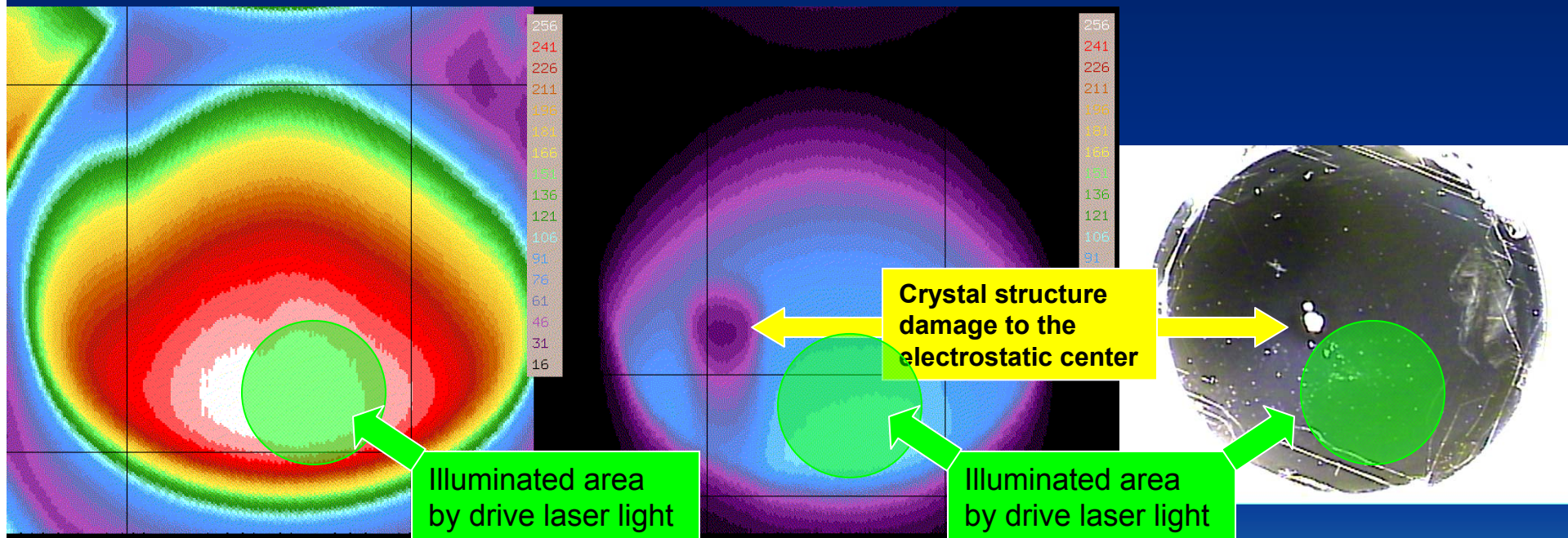
# High-current Operation



Courtesy of C. Hernandez-Garcia

# Ion Back-bombardment

Positive ions accelerated by the electrostatic field strike the cathode surface causing a drop in quantum efficiency and damages to the crystal structure.



QE of a new GaAs photocathode is 5-7%

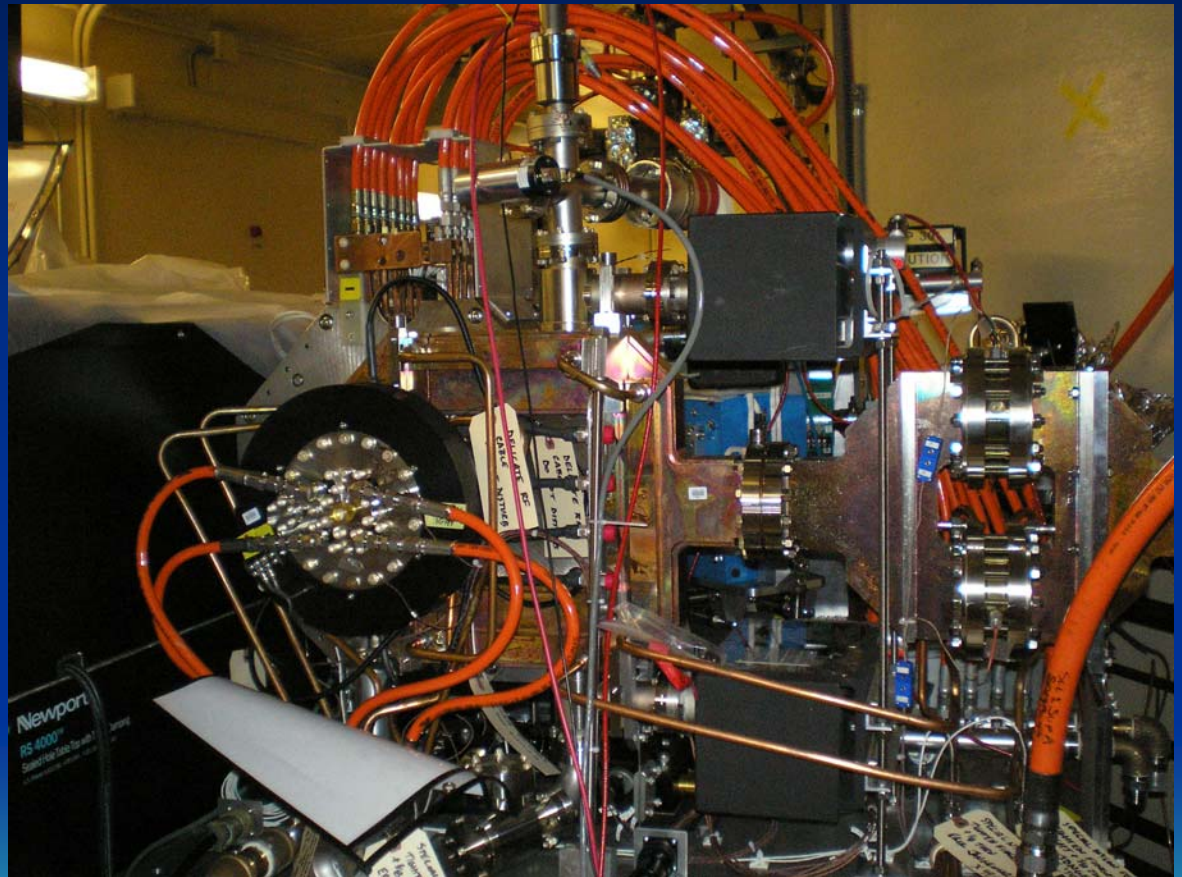
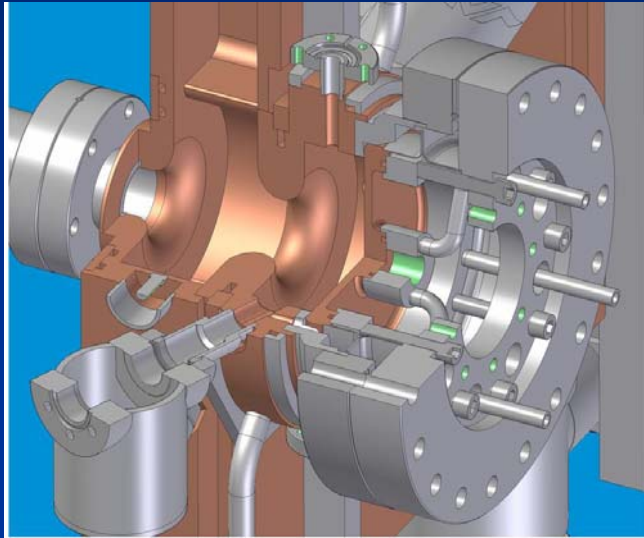
QE of a used GaAs cathode drops to 1%

Damages on GaAs wafer after a high-current run

Courtesy of C. Hernandez-Garcia

# Normal-Conducting RF Injector

## LCLS S-band NCRF Gun



Courtesy of D. Dowell

# Schematic of an NCRF Injector

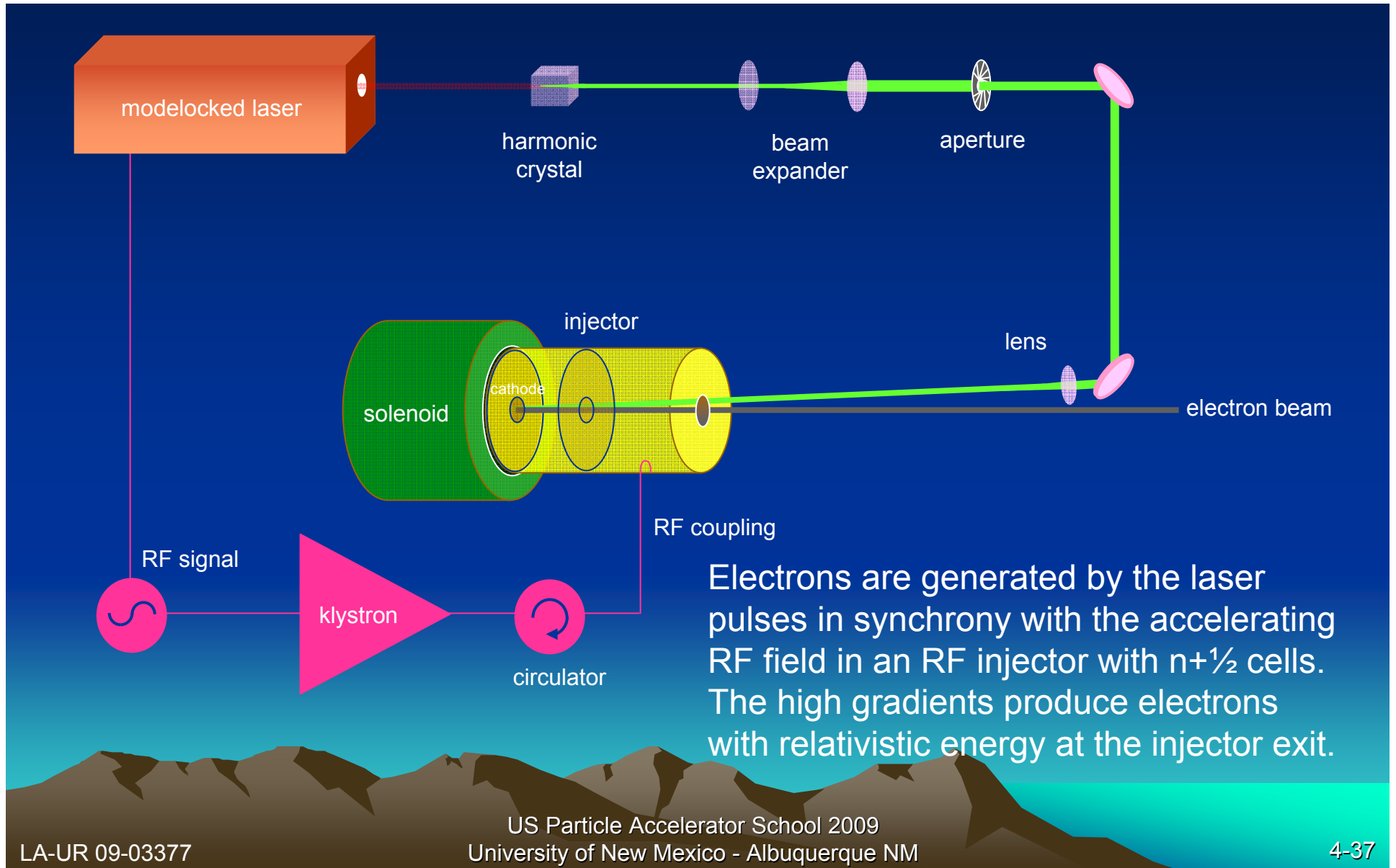
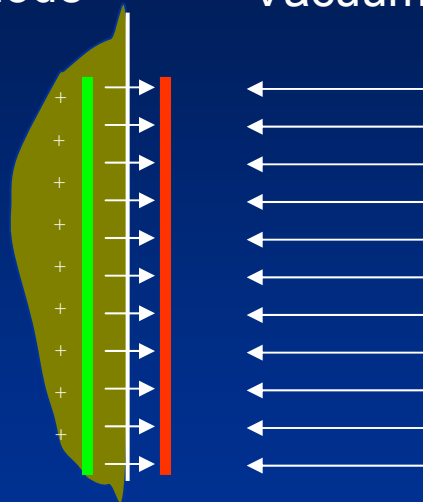


# Image Charge Effects

Cathode

Vacuum



$$\phi_0 = 12^\circ$$

Applied RF field

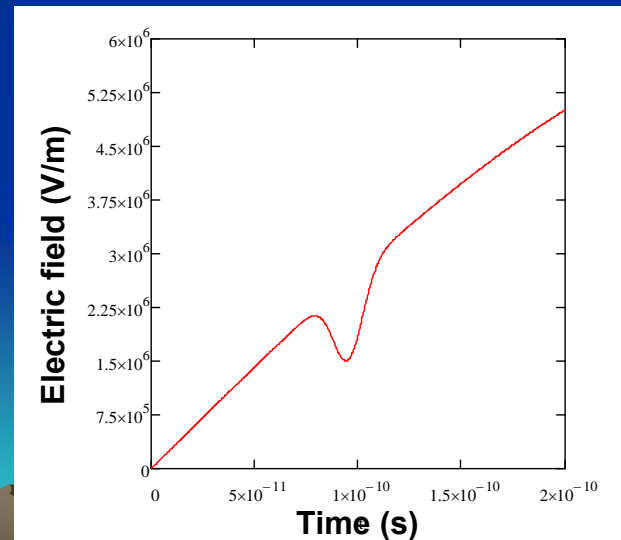
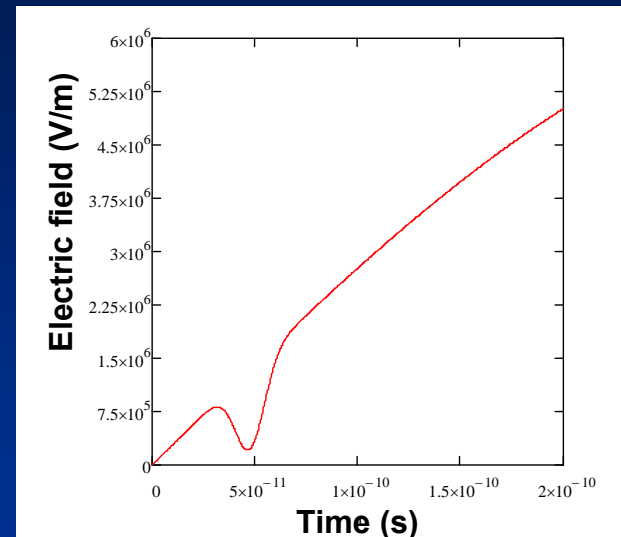
$$E_z = E_0 \sin(\omega t + \phi_0)$$

Image charge field

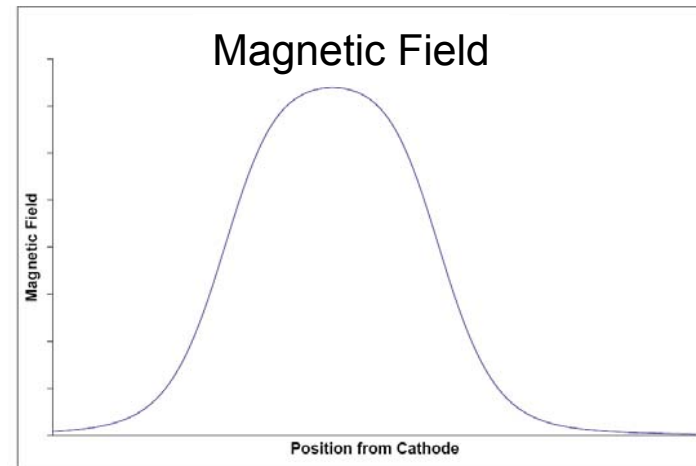
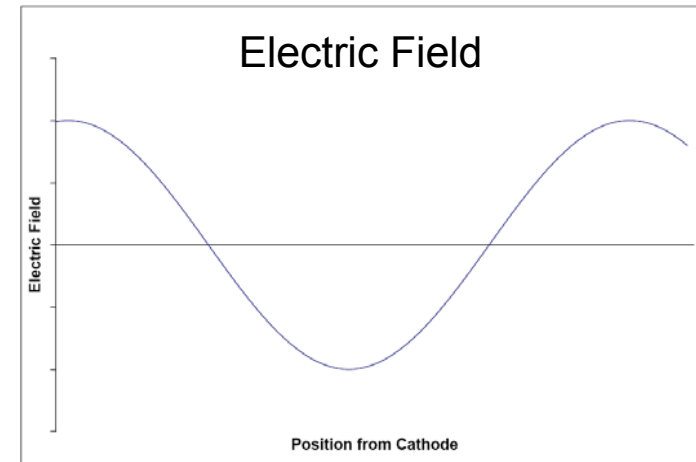
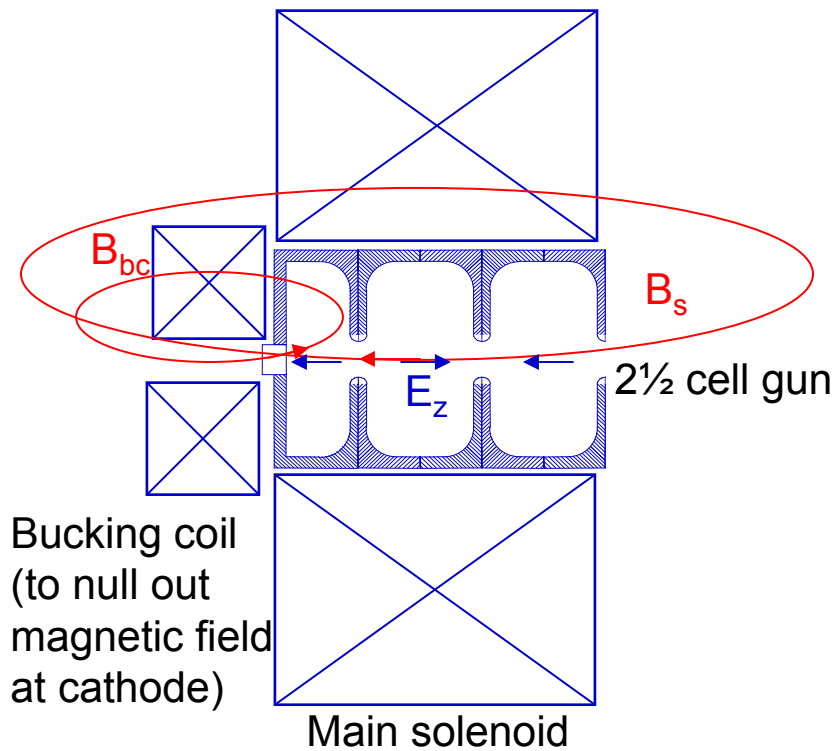
$$E_{IC} = \frac{q}{\epsilon_0 \pi r^2}$$

$$\phi_0 = 24^\circ$$

For 1 nC and 0.5 cm radius, the image charge field is 1 MV/m. The applied RF field at launch phase has to exceed the image charge field.



# Electric and Magnetic Fields



# Beam Envelope Equation

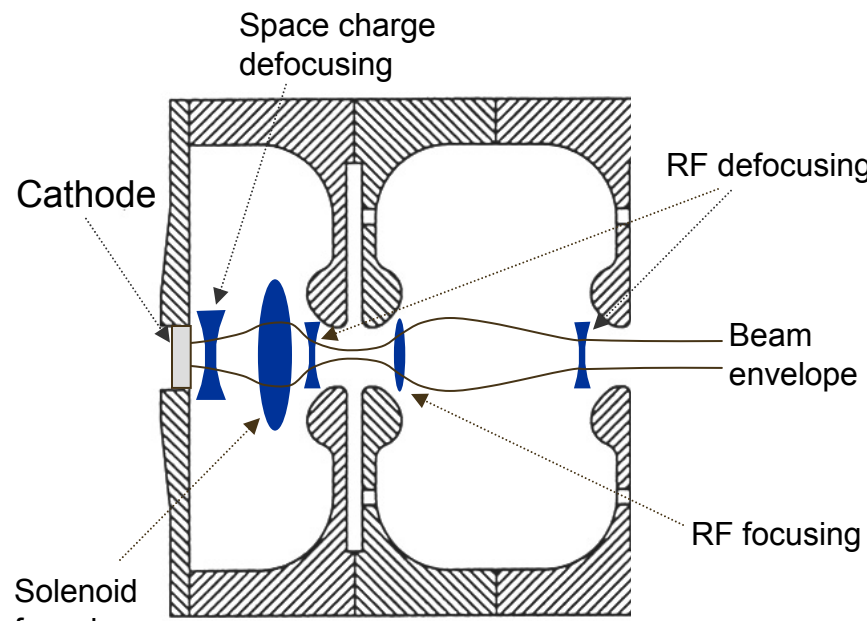
Electron beam envelope equation in an RF injector

$$\sigma'' + \sigma' \left( \frac{\gamma'}{\beta\gamma} \right) + k_B^2 \sigma - \frac{I}{\beta^3 \gamma^3 I_0 \sigma} - \frac{e}{\beta \gamma m c^2} (E_r - v_z B_\theta) - \frac{\epsilon_T^2}{\beta^2 \gamma^2 \sigma^3} = 0$$

Acceleration damping  
 Solenoidal focusing  
 Space charge expansion  
 RF focusing & defocusing due to radial electric field  
 RF focusing due to azimuthal magnetic field  
 Thermal emittance

The beam envelope equation describes the forces acting on the beam envelope radius. If the signs of the terms on the left hand side are positive, the beam sees focusing forces. If the signs of the terms on the left hand side are negative, the beam sees defocusing forces.

# Emittance Growth in RF Injectors



Space charge defocusing  
 Cathode  
 Solenoid focusing  
 RF defocusing  
 Beam envelope  
 RF focusing

*Space-charge induced emittance*  

$$\varepsilon_{n,sc} = \frac{I}{\gamma I_A \left( \frac{3\sigma_r}{\sigma_z} + 5 \right)}$$

*RF induced emittance*  

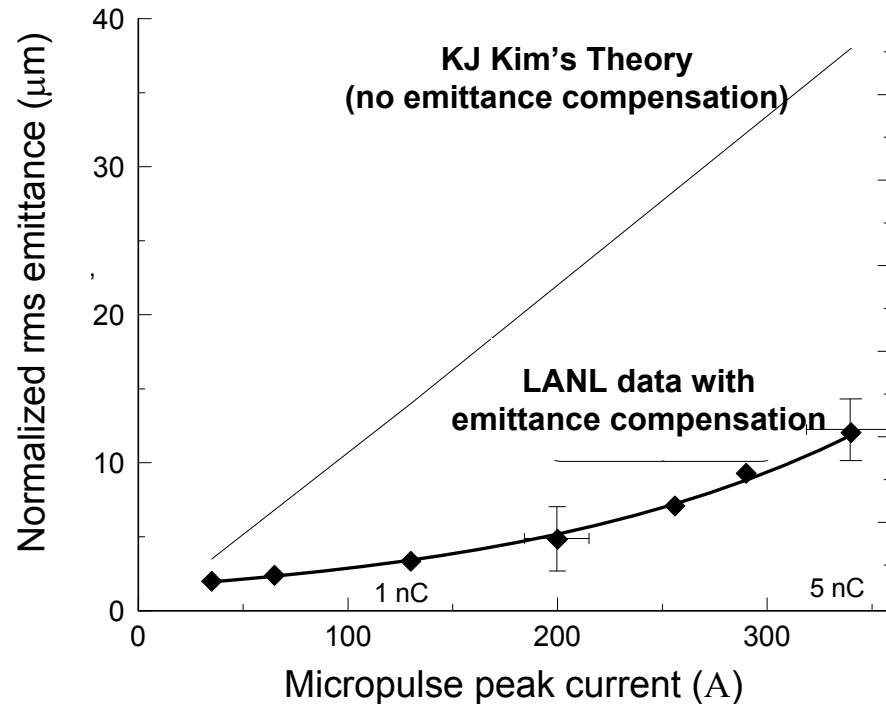
$$\varepsilon_{n,RF} = \gamma k_{RF}^2 \sigma_r^2 \sigma_z^2$$

*Thermal emittance*  

$$\varepsilon_{n,thermal} = \sigma_r \sqrt{\frac{kT}{mc^2}}$$

- Space charge      Space charge is reduced by using large radius, high gradient, and long electron bunch.
- RF                    RF effects are reduced with small radius, solenoid focusing, short electron bunch, and low frequency.
- Thermal            Reduced with small radius, semiconductor cathodes

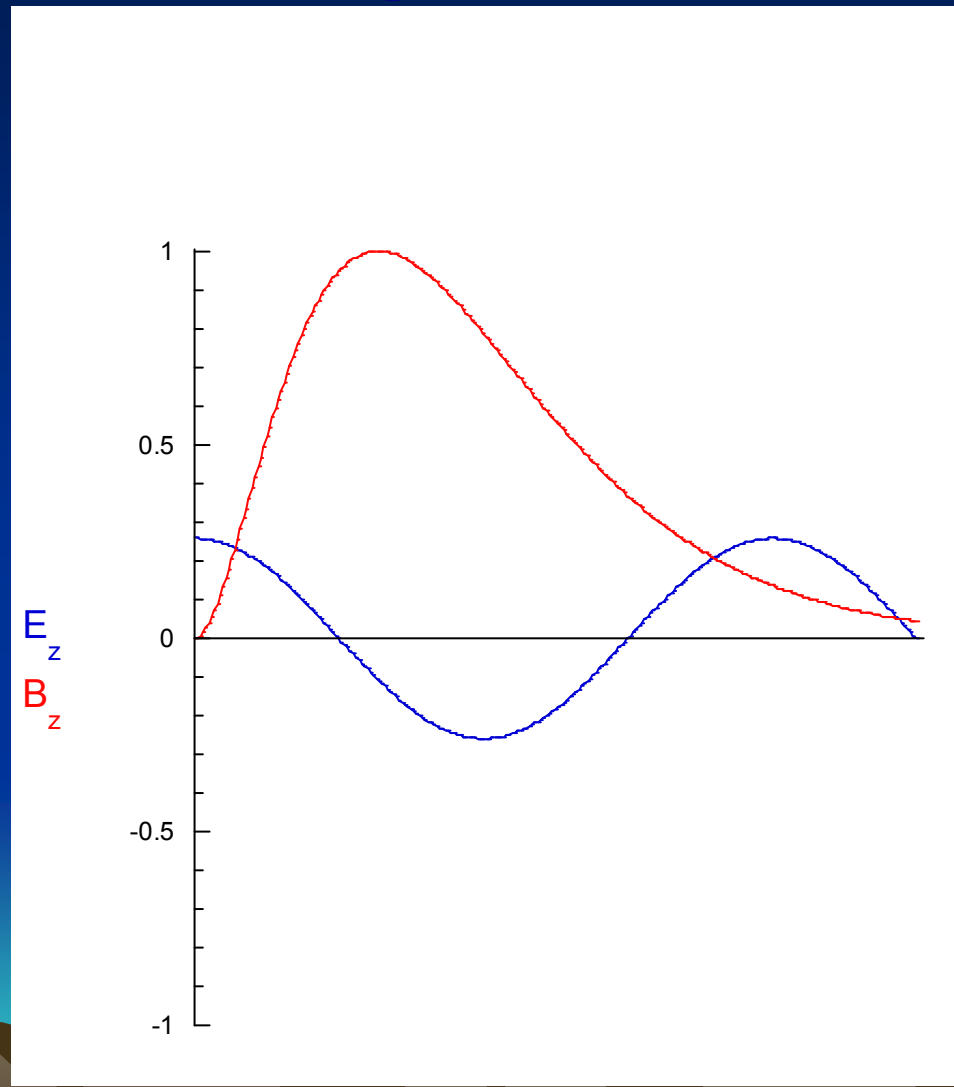
# Emittance vs Bunch Charge and Current



The experimentally measured emittance is better than theoretical predictions because KJ Kim's theory does not account for emittance compensation effects. Note the nonlinear increase in normalized emittance with charge.

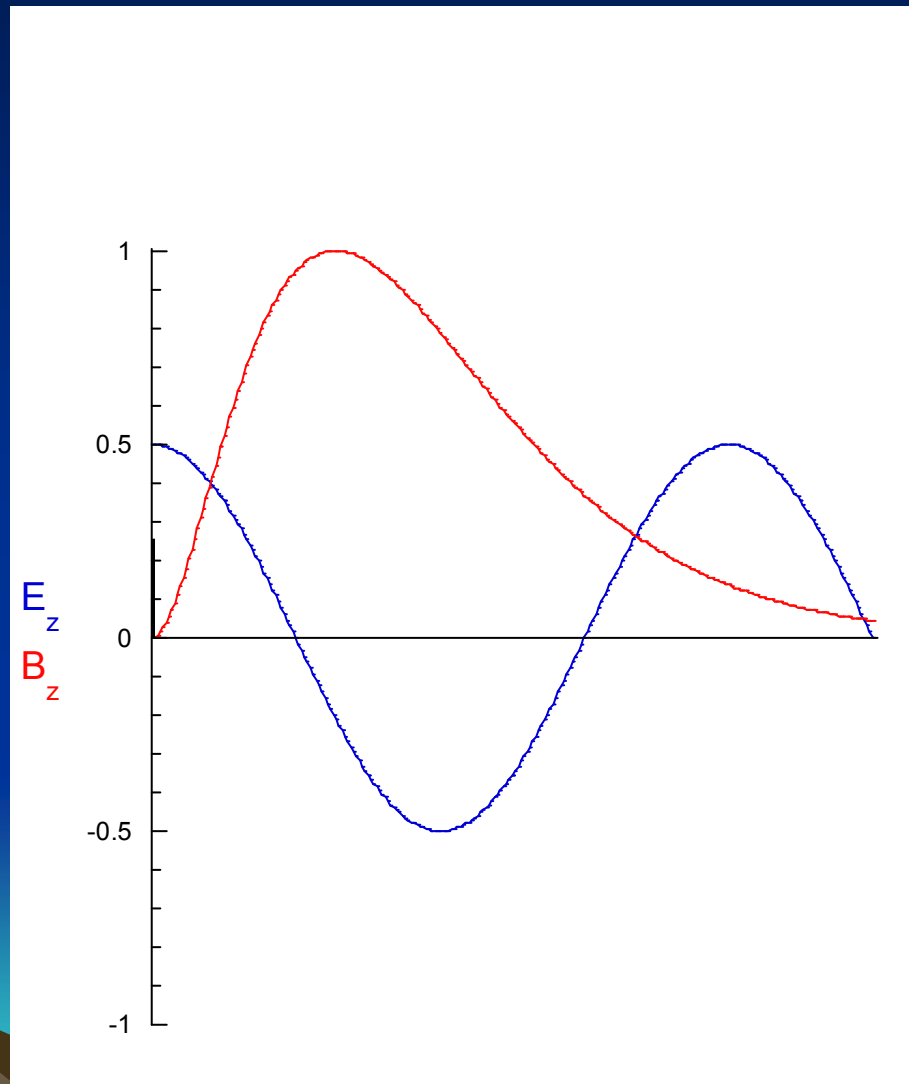
Courtesy of P. O'Shea

# Beam Dynamics in an RF Injector with Magnetic Focusing



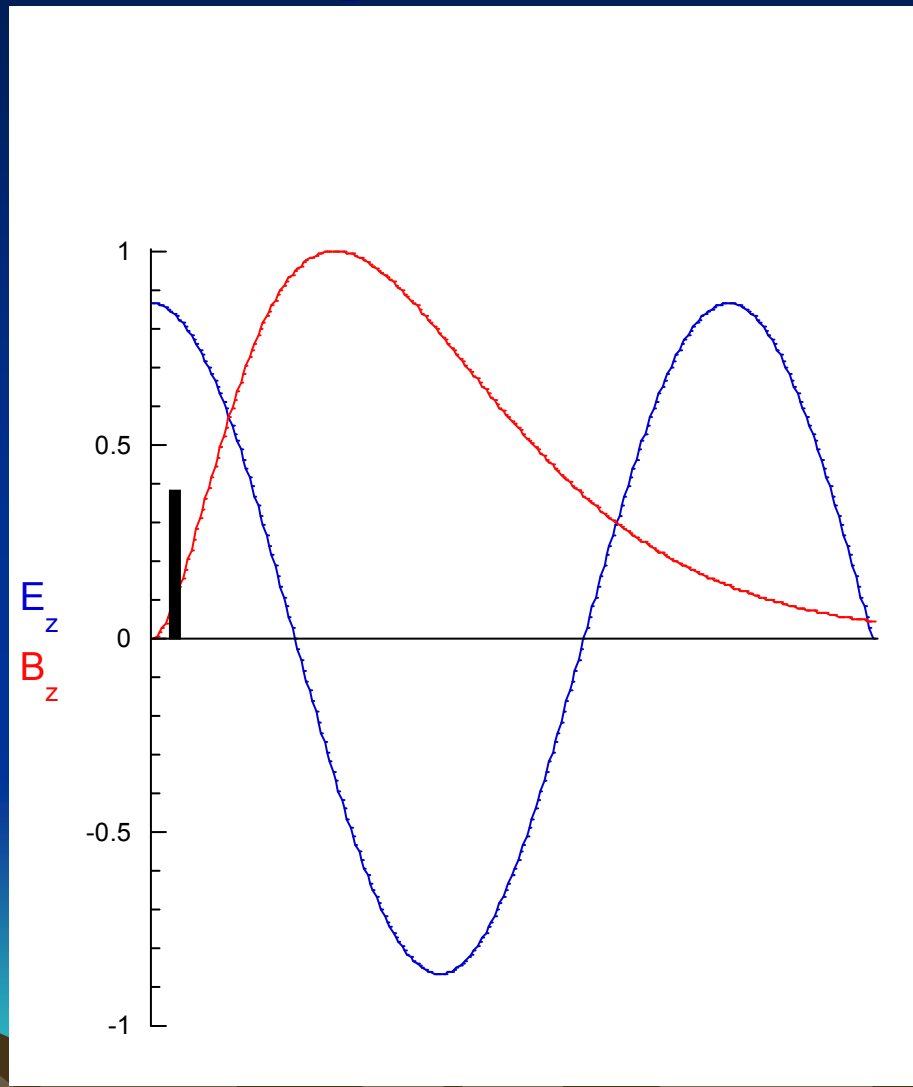
$$\Phi = \pi/12$$

# Beam Dynamics in an RF Injector with Magnetic Focusing



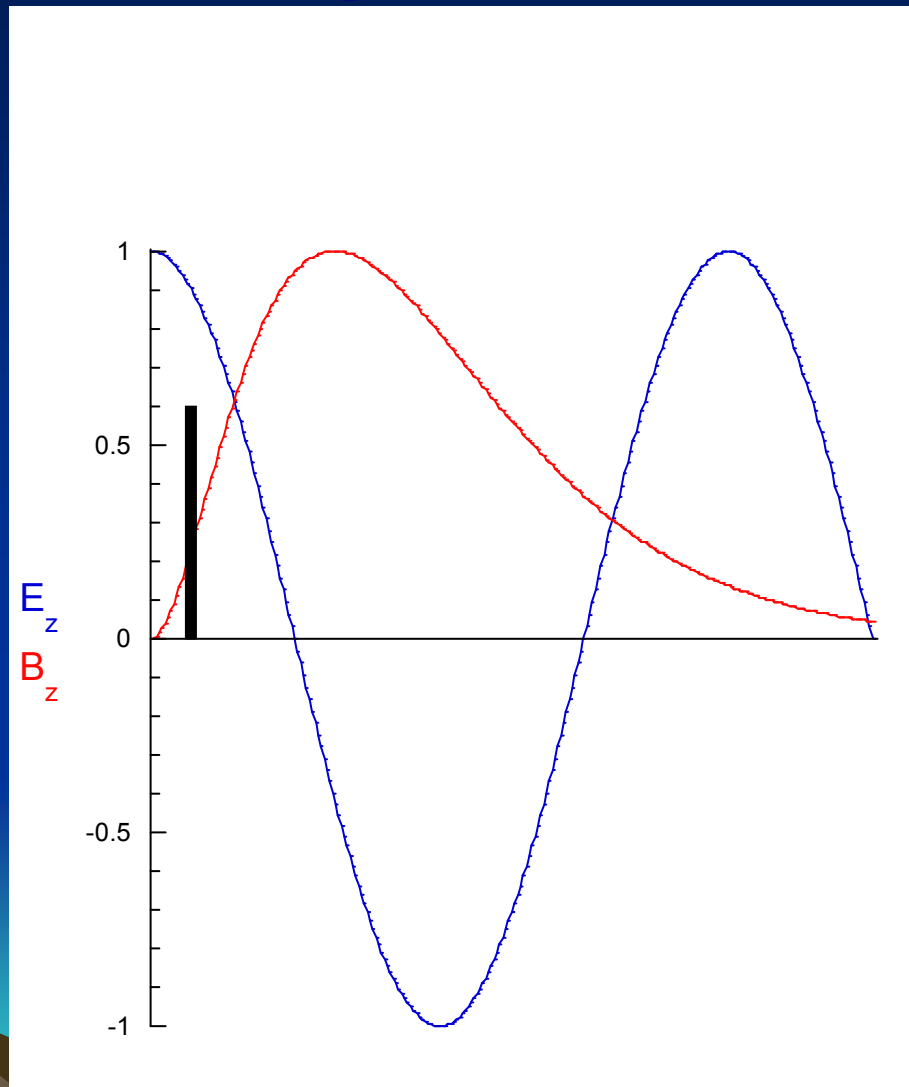
$$\Phi = \pi/6$$

# Beam Dynamics in an RF Injector with Magnetic Focusing



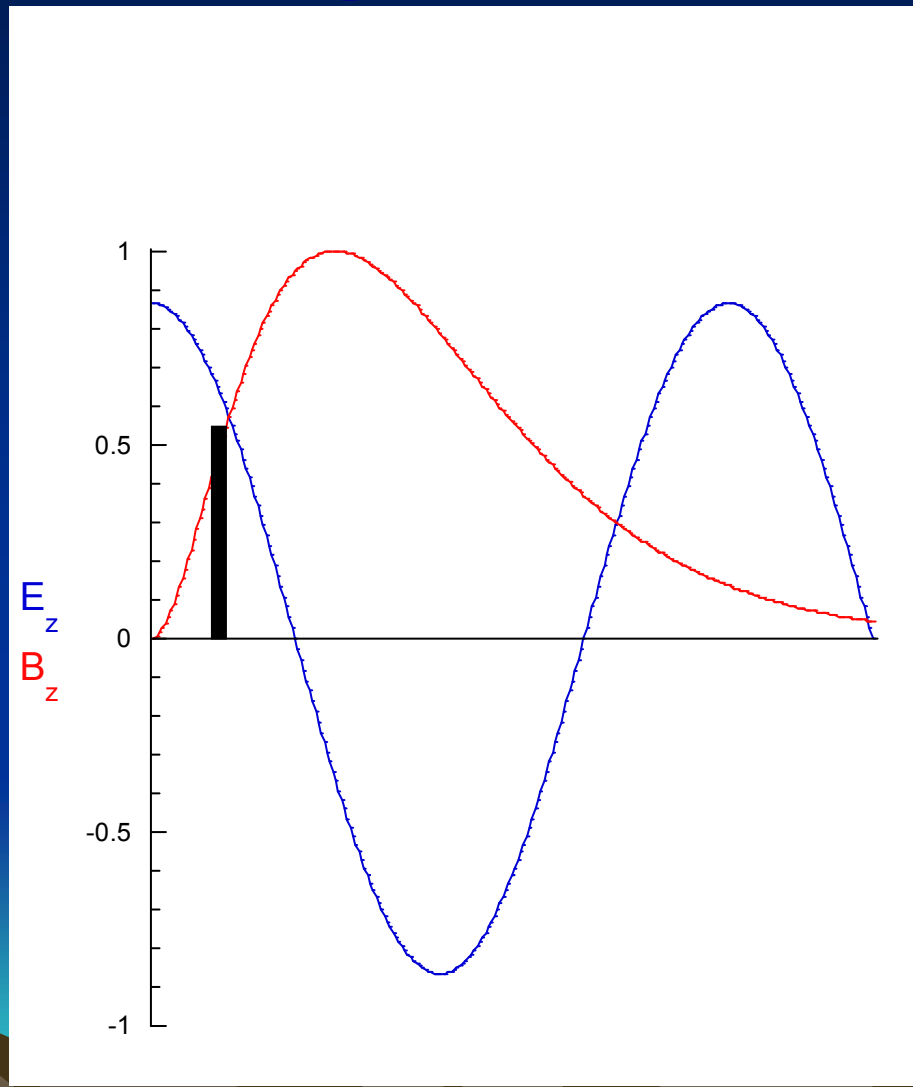
$$\Phi = \pi/3$$

# Beam Dynamics in an RF Injector with Magnetic Focusing



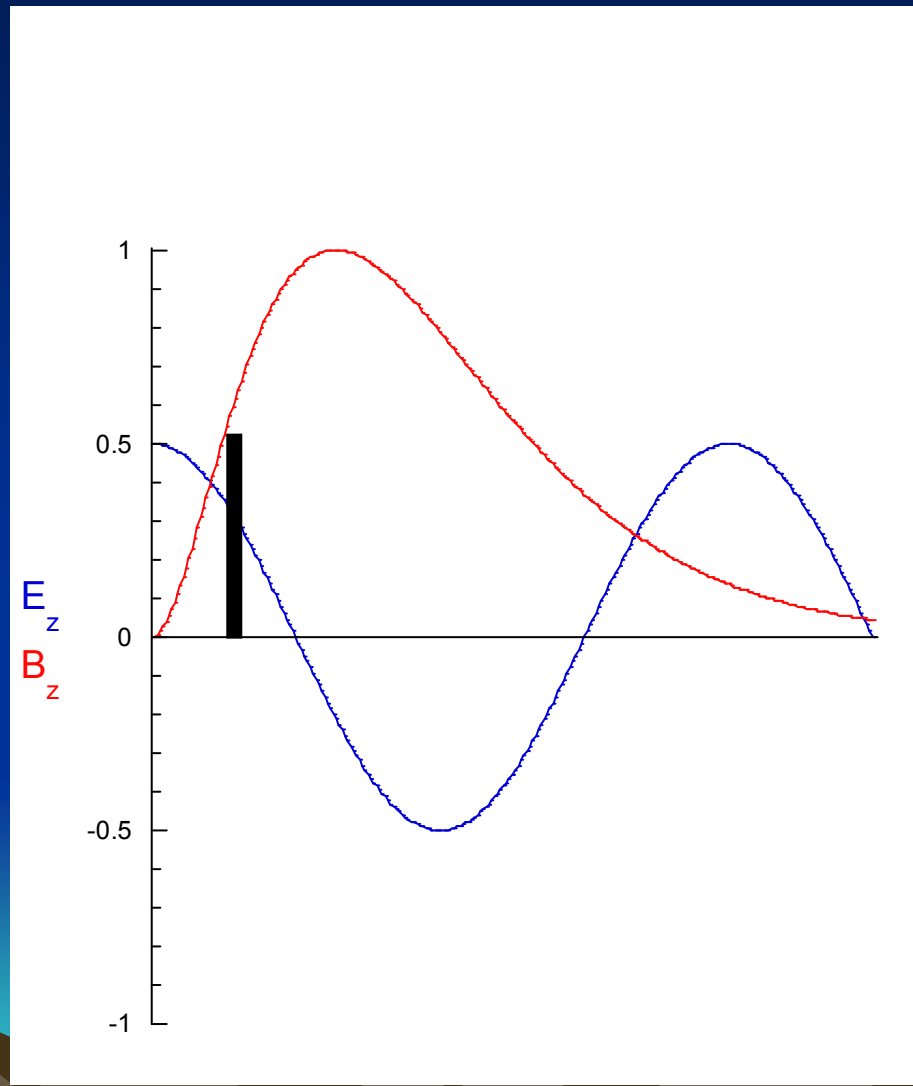
$$\Phi = \pi/2$$

# Beam Dynamics in an RF Injector with Magnetic Focusing



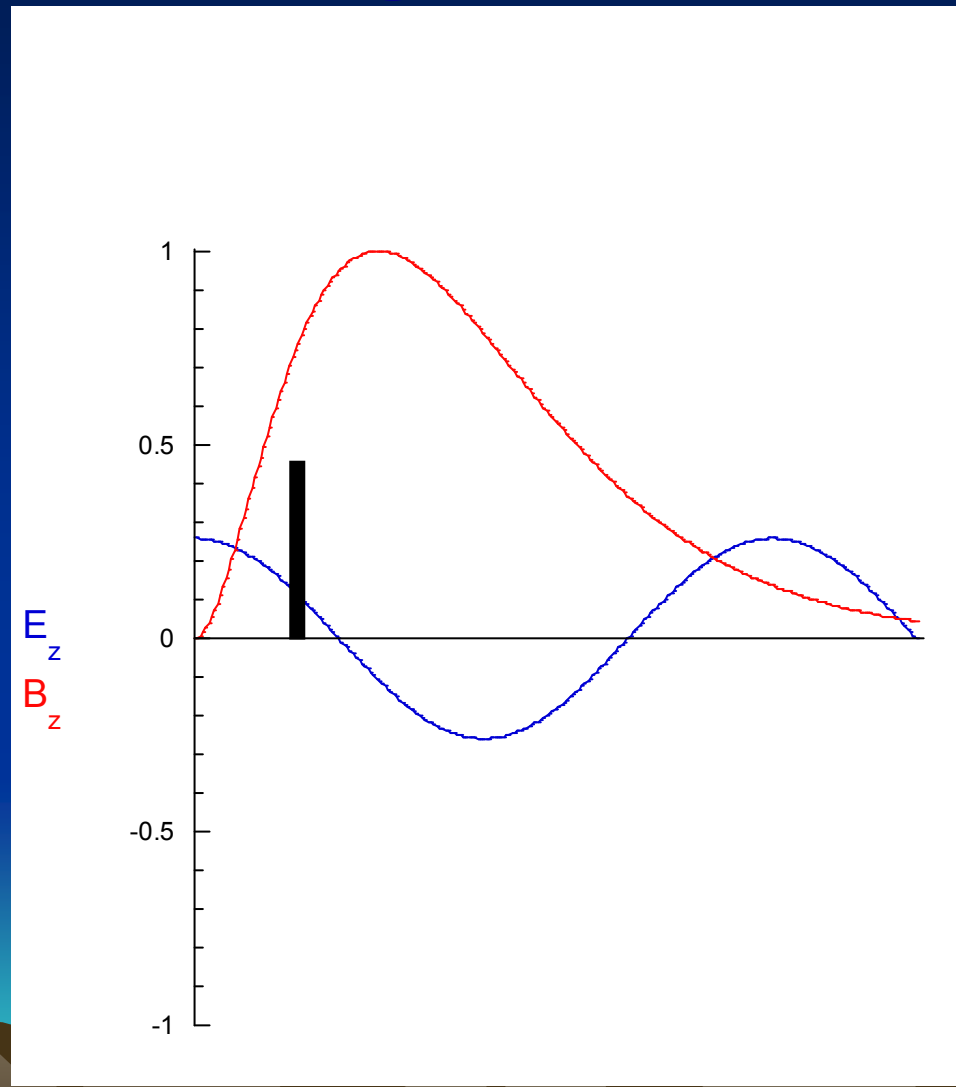
$$\Phi = 2\pi/3$$

# Beam Dynamics in an RF Injector with Magnetic Focusing



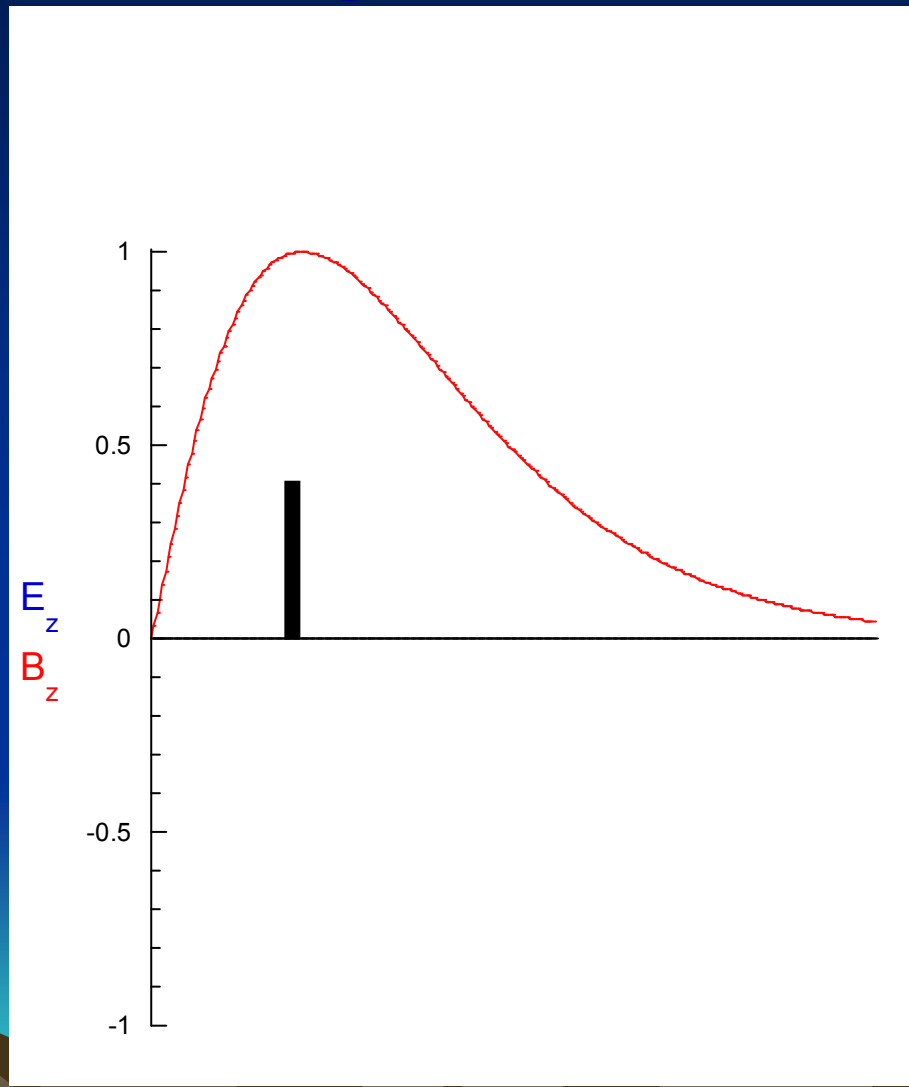
$$\Phi = 5\pi/6$$

# Beam Dynamics in an RF Injector with Magnetic Focusing



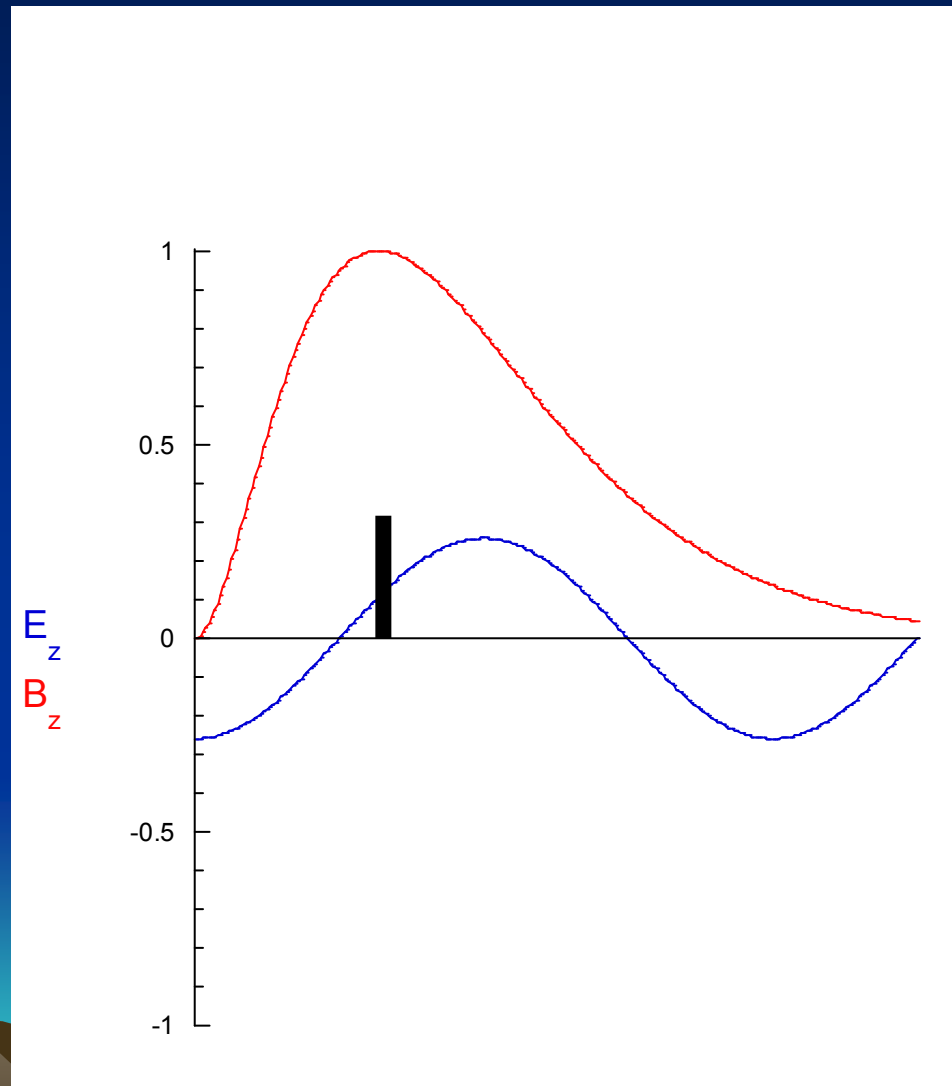
$$\Phi = 11\pi/12$$

# Beam Dynamics in an RF Injector with Magnetic Focusing



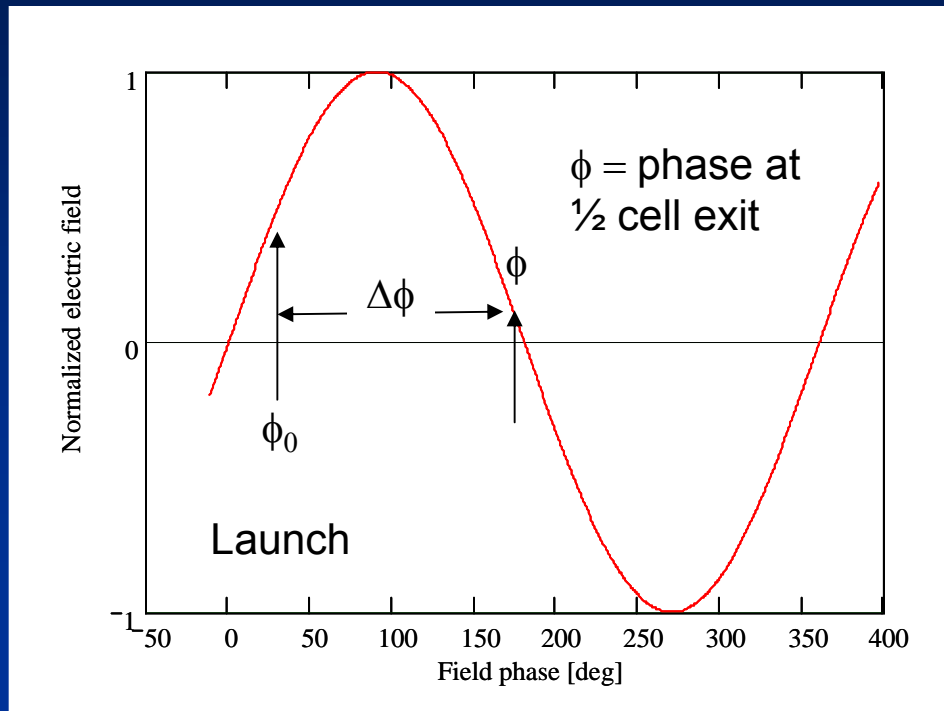
$$\Phi = \pi$$

# Beam Dynamics in an RF Injector with Magnetic Focusing



$$\Phi = 13\pi/12$$

# Single-Particle Equation of Motion



On-axis accelerating field

$$E(t) = E_0 \cos(kz) \sin(\omega t + \phi_0)$$

Change independent variable

$$\zeta = kz$$

Energy evolution

$$\frac{d\gamma}{d\zeta} = \alpha [\sin \phi + \sin(\phi + 2\zeta)]$$

Phase evolution

$$\phi = \omega t - kz + \phi_0 = \beta^{-1}\zeta - \zeta + \phi_0$$

$$\beta^{-1} = \frac{c}{v} = \frac{\gamma}{\sqrt{\gamma^2 - 1}}$$

$$\frac{d\phi}{d\zeta} = \frac{\gamma}{\sqrt{\gamma^2 - 1}} - 1$$

Dimensionless gradient

$$\alpha = \frac{eE_0}{2km_0c^2}$$

RF wavenumber

$$k = \frac{2\pi}{\lambda_{RF}}$$

# Solution to Single-particle EOM

Approximate solution for energy

$$\tilde{\gamma} = 1 + 2\alpha kz \sin \phi_0$$

where

$$\alpha = \frac{eE_0}{2km_0c^2}$$

Plug the approximate  $\gamma$  into the phase equation and integrate

$$\phi = \frac{1}{2\alpha \sin \phi_0} \left[ \sqrt{\tilde{\gamma}^2 - 1} - (\tilde{\gamma} - 1) \right] + \phi_0$$

Plug the phase solution into the energy equation (without 2<sup>nd</sup> term) and integrate

$$\gamma = 1 + \alpha \left[ kz \sin \phi_0 + \frac{1}{2} (\cos \phi - \cos(\phi + 2kz)) \right]$$

To minimize emittance, select the launch phase such that the beam exits the first cell at  $\phi = \pi$

$$(\pi - \phi_0) \sin \phi_0 = \frac{1}{2\alpha}$$

Numerical examples for LCLS

$$E_0 = 100 \text{ MV/m}$$

$$k = 2\pi/\lambda = 2\pi/(10.5 \text{ cm})$$

$$\alpha = 1.635$$

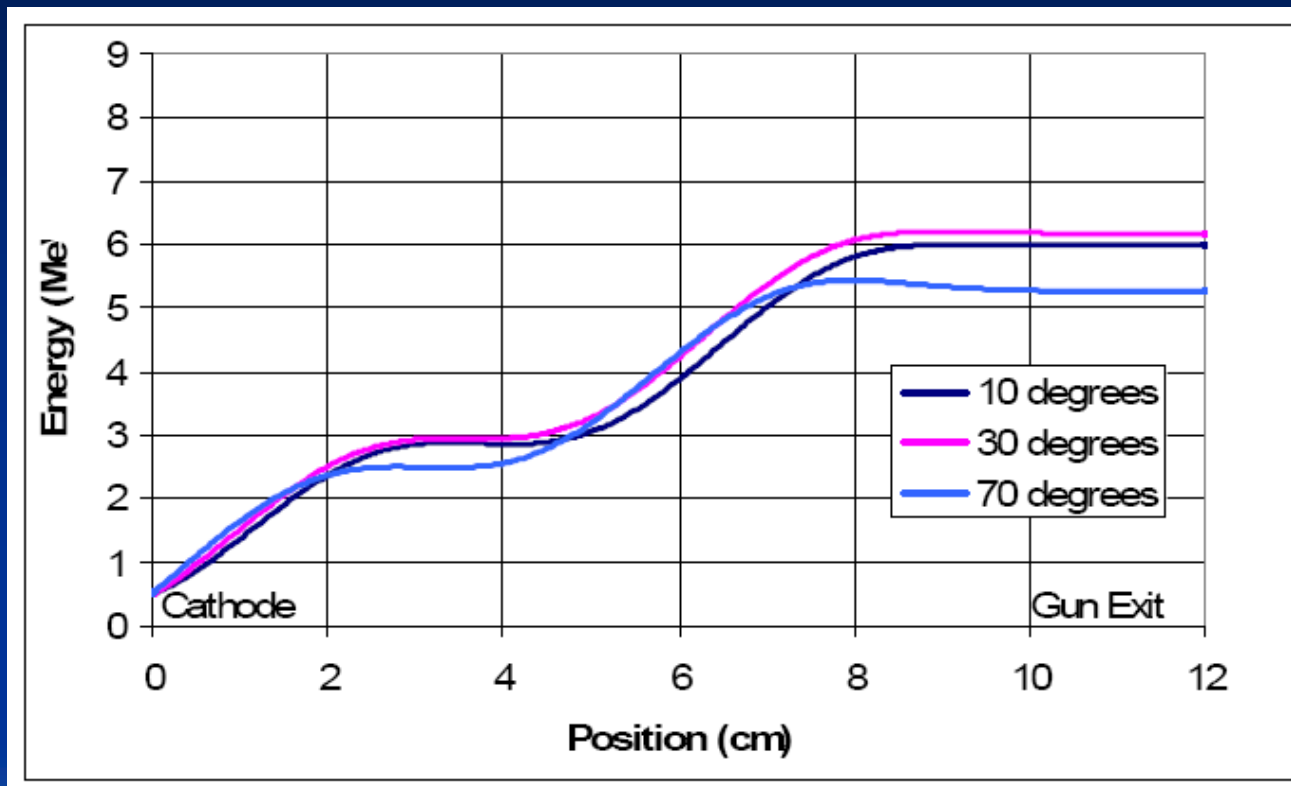
Optimum launch phase

$$\phi_0 = 6^\circ$$

Energy at first cell exit

$$E = 2.1 \text{ MeV}$$

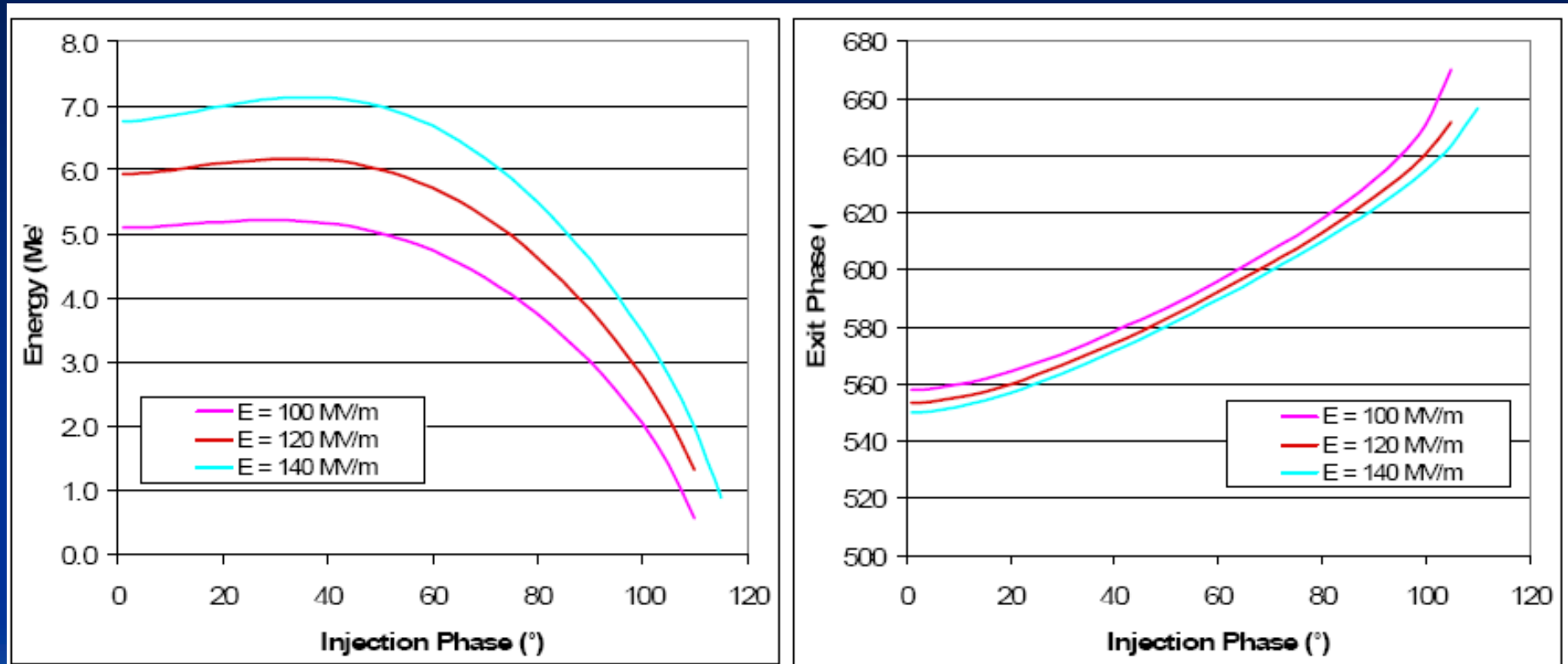
# Energy Gain



Numerical calculations yield a beam energy that is higher than KJ Kim's analytical predictions. The beam is relativistic at the end of the 1<sup>st</sup> cell.

Courtesy of J. Schmerge

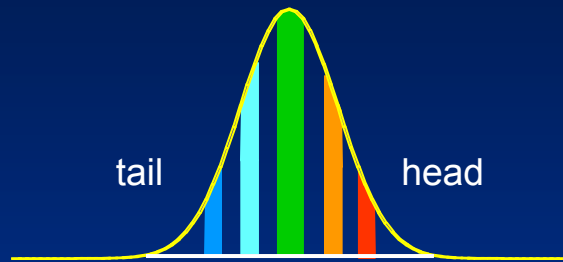
# Energy and Exit Phase vs Launch Phase



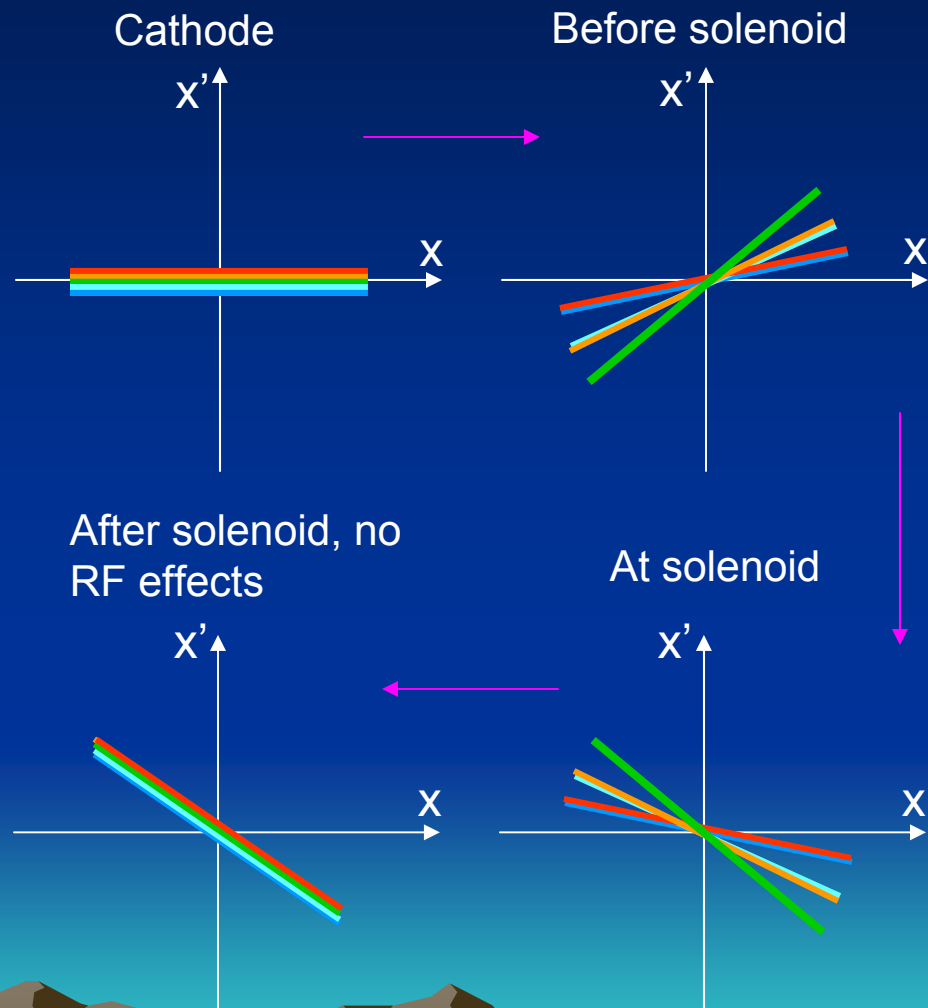
The beam energy at the exit of the LCLS 1½-cell gun is linearly proportional to the cavity gradient. The beam energy is almost independent of launch phase up to a launch phase of 50°.

Courtesy of J. Schmerge

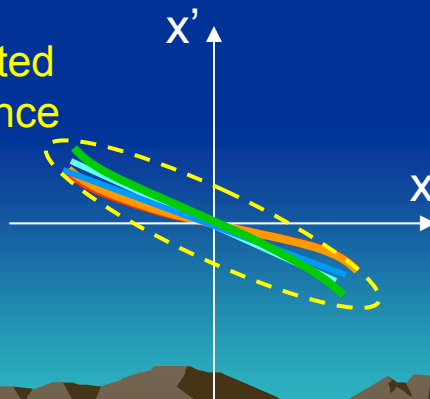
# Emittance Compensation (Carlsten's) Theory



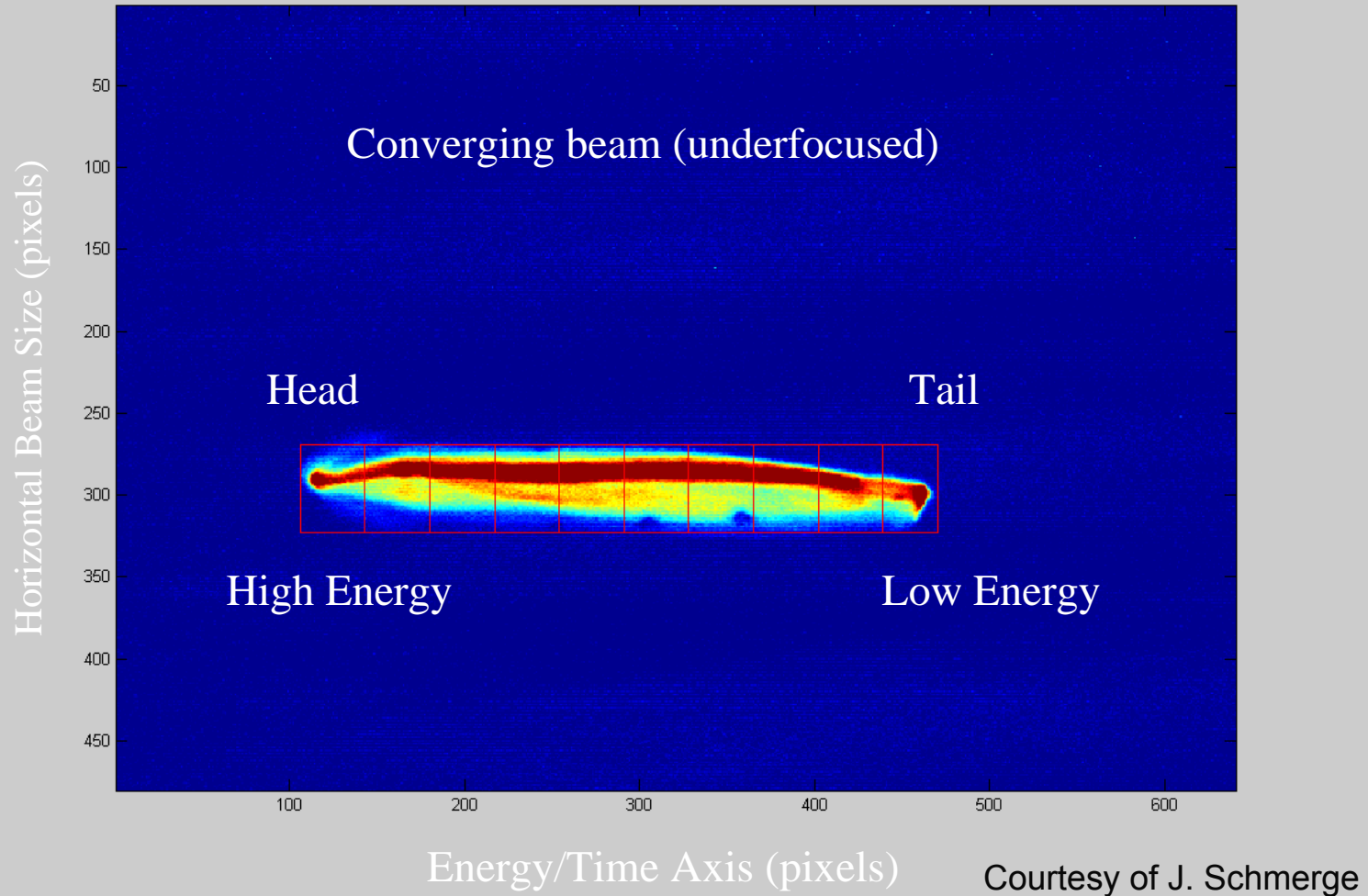
Electron bunch is sliced into  $N$  axial slices, each having its own phase space ellipse



Projected emittance



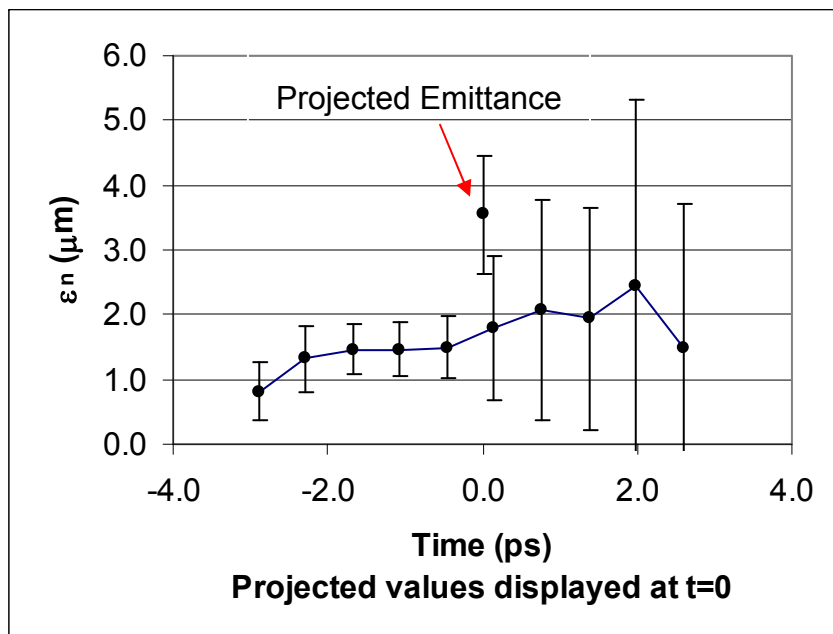
# Slice Emittance



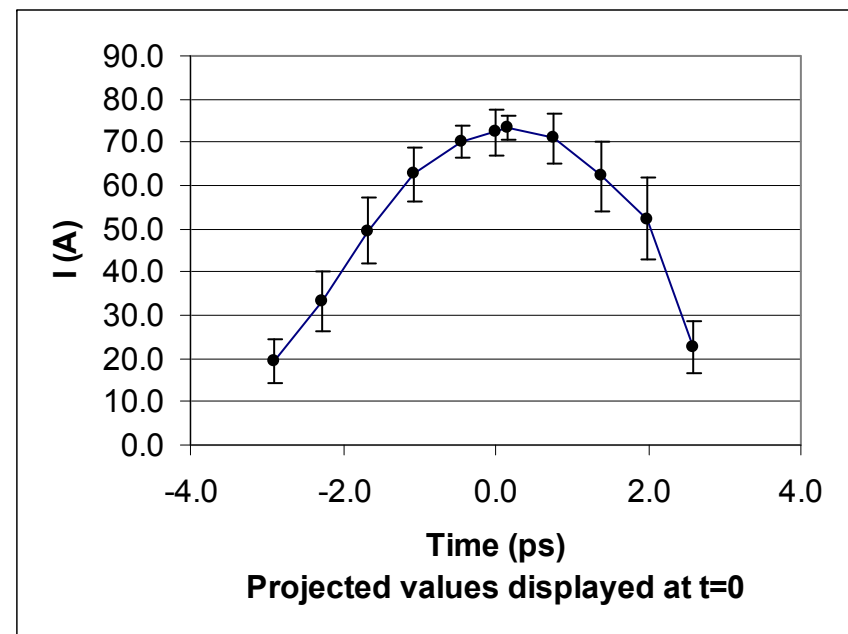
# Measured Slice Emittance & Current

Courtesy of J. Schmerge

Slice Normalized Emittance



Slice Peak Current



The slice emittance is approximately one-half the projected emittance (emittance of all slices projected onto  $x'-x$  phase space). The smaller slice emittance translates into better FEL performance (e.g. shorter gain length).

# Invariant Envelope (Serafini-Rosenzweig's) Theory

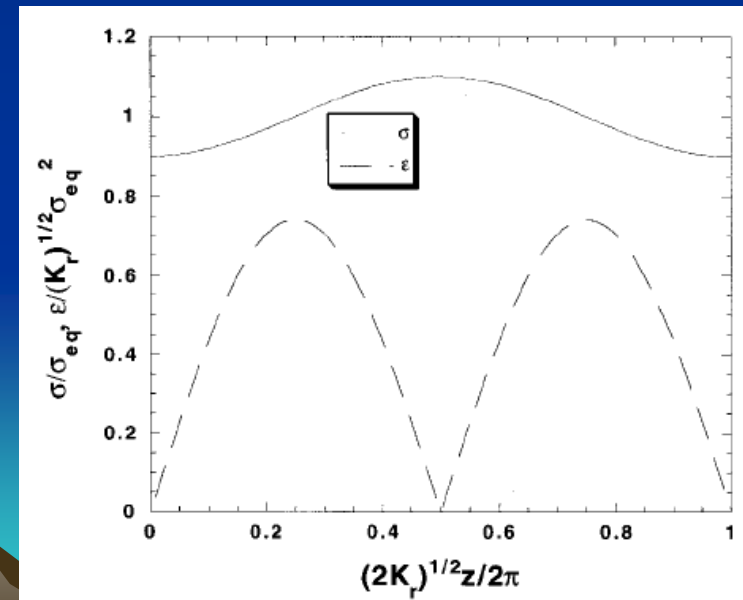
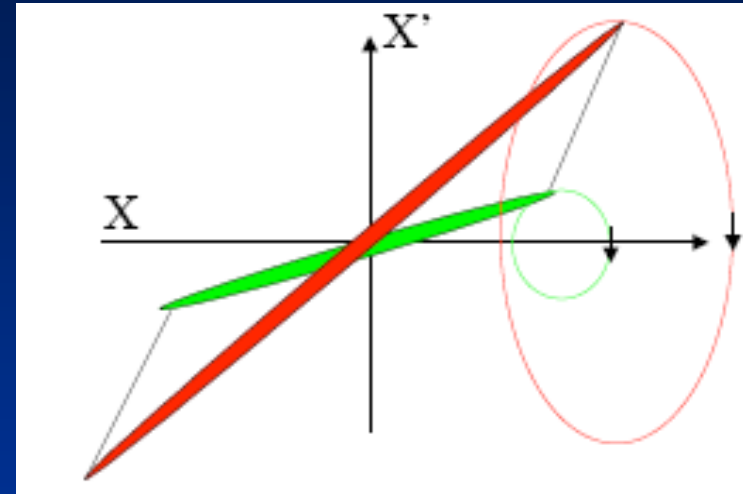
Perturbed trajectories oscillate around the equilibrium with the same frequency but with different amplitudes.

Invariant envelope corresponds to the matched beam envelope

$$\sigma_{inv} = \frac{2}{\gamma'} \sqrt{\frac{I}{3\gamma I_0}}$$

$$\sigma'_{inv} = \frac{1}{\gamma} \sqrt{\frac{2I}{3\gamma I_0}}$$

Match the beam to invariant envelope (however, this is not possible inside an RF gun).



# Invariant Envelope Oscillation in Linac

Electron beam envelope equation in the booster linac

$$\sigma'' + \sigma' \left( \frac{\gamma'}{\gamma} \right) + \left( \frac{\gamma''}{2\gamma} + \frac{1}{2} \left( \frac{\gamma'}{\gamma} \right)^2 + k_{RF}^2 \right) \sigma - \frac{\kappa}{\gamma^3 \sigma} - \frac{\epsilon_n^2}{\gamma^2 \sigma^3} = 0$$

Invariant envelope for space charge dominated beam

$$\hat{\sigma}_{sc} = \frac{1}{\gamma'} \sqrt{\frac{4\kappa}{3\gamma}}$$

where  $\kappa = \frac{I}{I_0}$

Invariant envelope for emittance dominated beam

$$\hat{\sigma}_{emit} = \sqrt{\frac{2\gamma\epsilon_n}{\sqrt{3}\gamma'}}$$

Transition energy  $\gamma = \frac{2}{\sqrt{3}\gamma'\epsilon_n} \frac{I}{I_0}$

Acceleration damps the plasma oscillation resulting in a steady-state emittance. The beam transitions from a space charge dominated beam at the linac entrance to emittance dominated beam at the exit. The transition energy is given above.

# Ferrario's Working Point

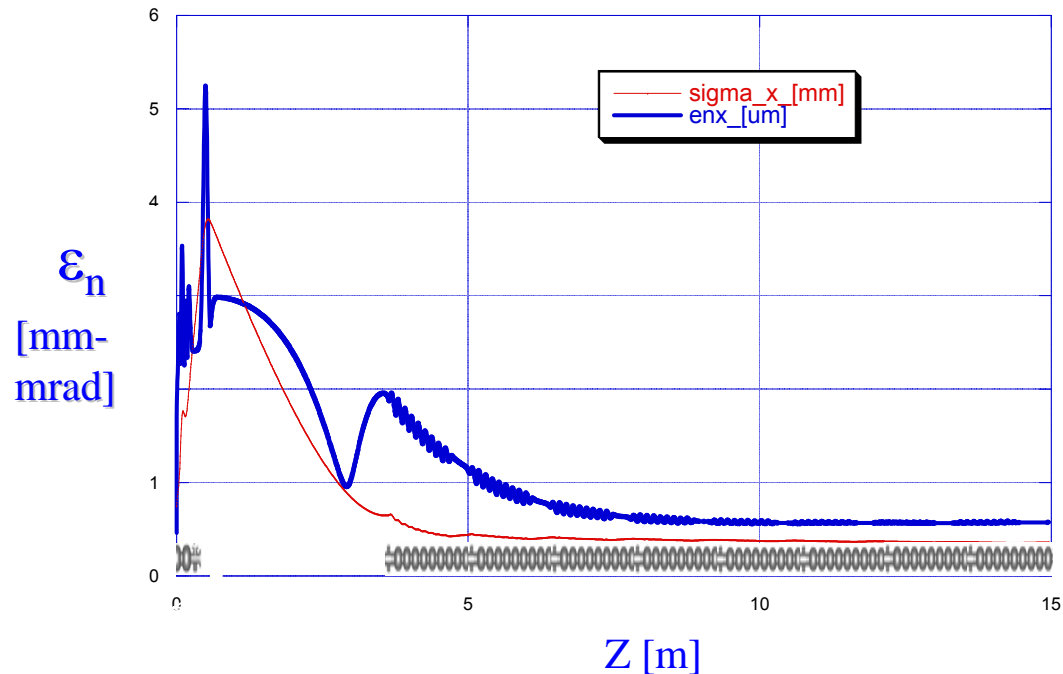
Matched beam  
rms radius

$$\sigma_{inv} = \frac{2}{\gamma'} \sqrt{\frac{I}{3\gamma_{entrance} I_0}}$$

Matched beam  
converging angle

$$\sigma'_{inv} = -\sqrt{\frac{2I}{3\gamma^3 I_0}}$$

Simulation for an L-band photoinjector

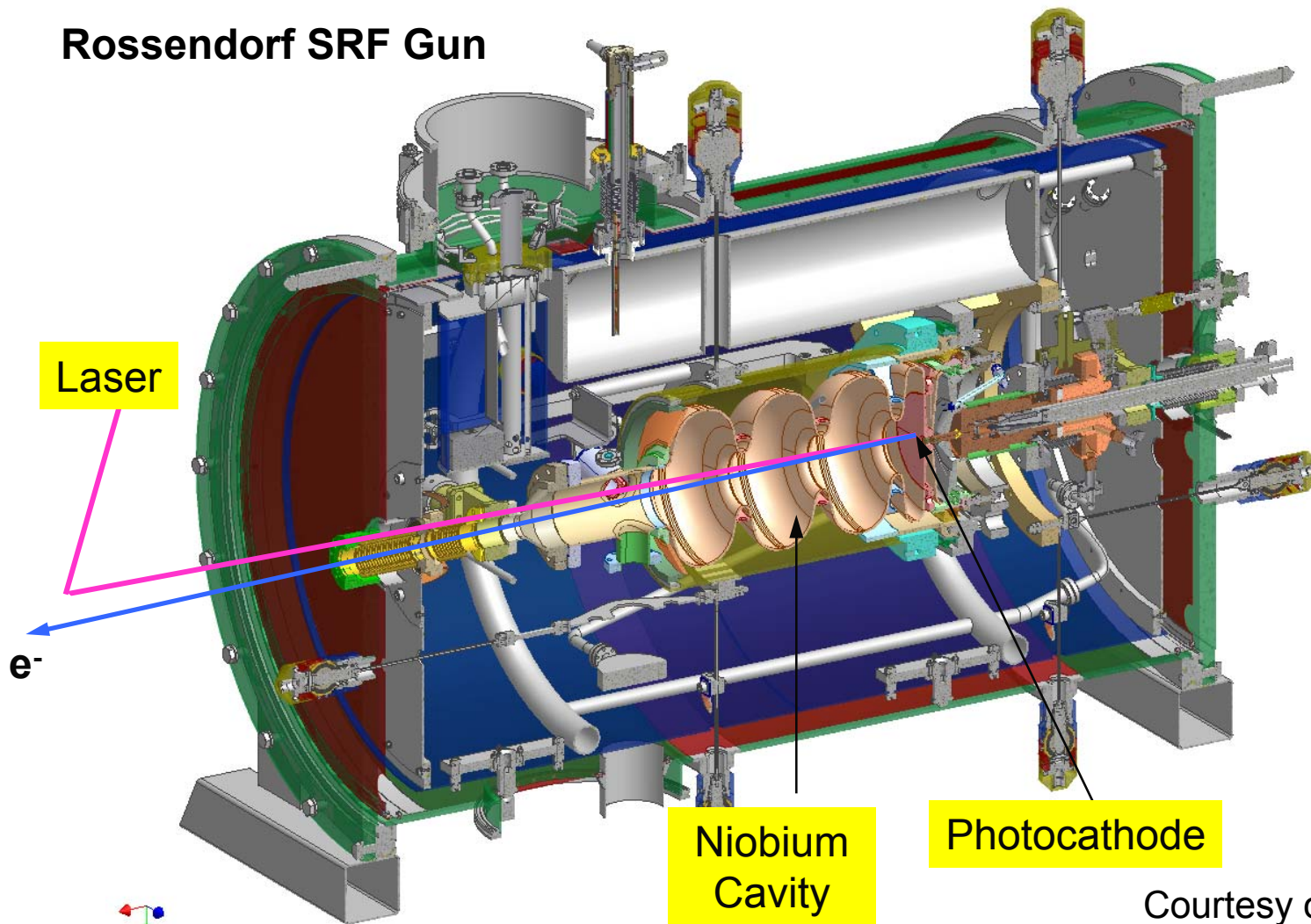


Courtesy of M. Ferrario

The beam is matched into the booster whose entrance is located between two emittance minima. Plasma oscillation is damped and the beam emittance asymptotically approaches an even lower emittance at very large  $z$ .

# Superconducting RF Injectors

Rossendorf SRF Gun



Courtesy of J. Teichert

# Pros and Cons of SRF Injectors

## *Pros*

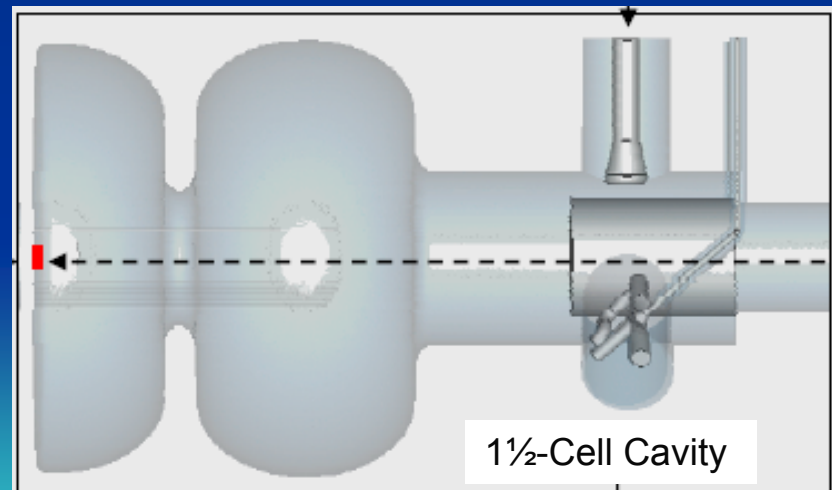
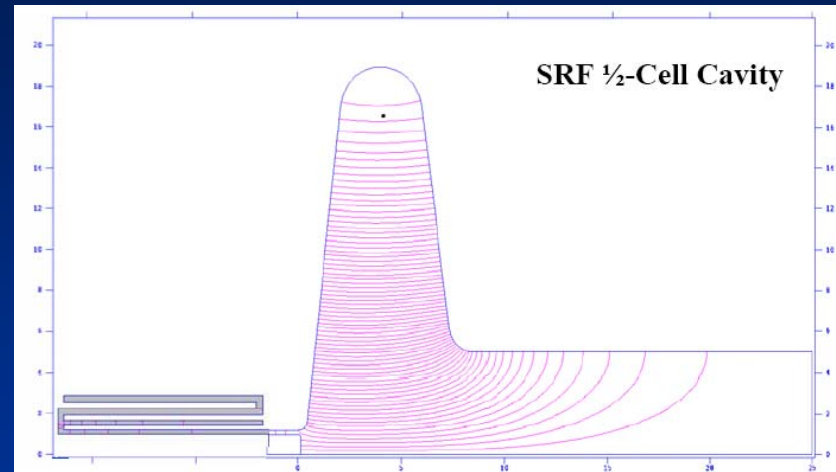
- Potentially high gradients in cw operation
- Potentially high quality electron beams thanks to high gradients
- Very efficient use of RF in cw operation
- Good vacuum (cryo pumping)

## *Cons*

- Presence of cathodes in the SRF cavity reduces the cavity Q
- Unable to accept solenoid fields inside the injector to perform emittance compensation
- If low-QE superconducting cathodes are used, high-power UV lasers can warm SRF surfaces
- If NEA cathodes are used, cesium contamination may increase risks of multipacting and field emission

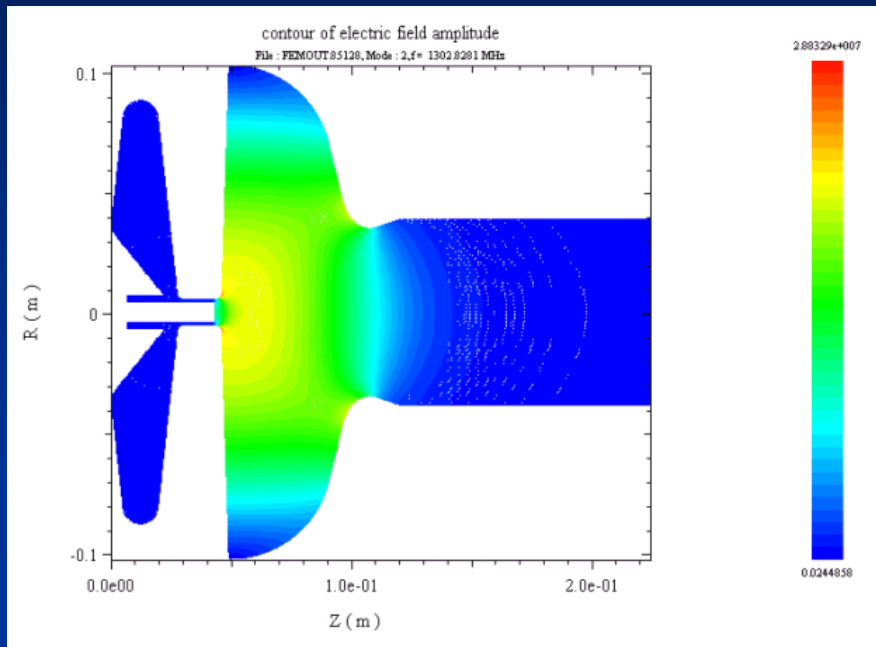
# Options for SRF Injectors

- Number of cells
  - $\frac{1}{2}$  cell SRF injector
  - $n+\frac{1}{2}$  cell SRF injector
- Cavity shapes
  - Triangular
  - Low-loss
  - Re-entrant
  - Quarter-wave
- Cathodes
  - Normal-conducting cathodes
    - Lead
    - Niobium
  - Superconducting cathodes

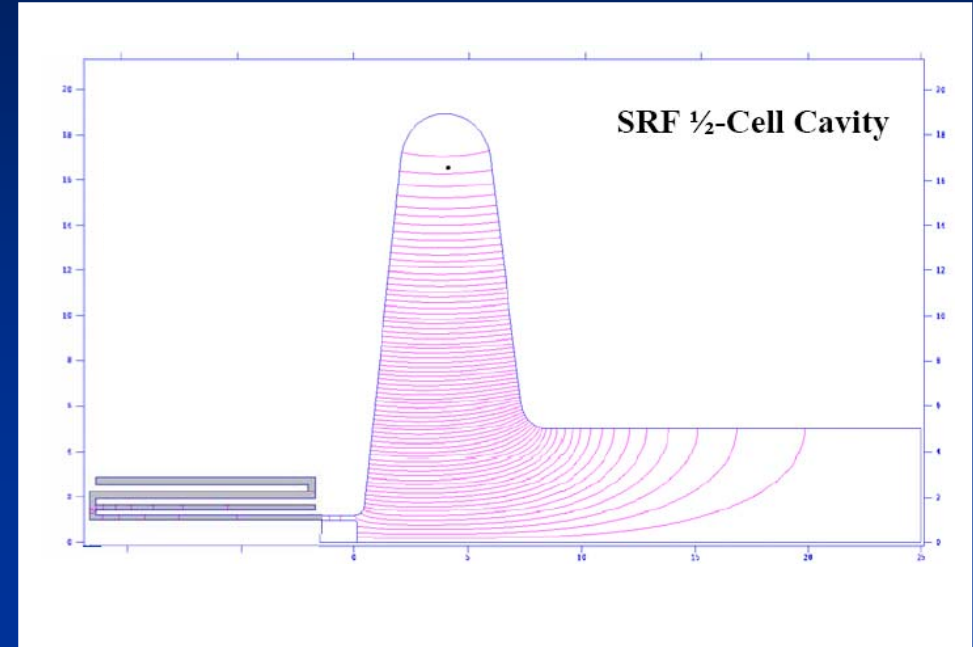


# Cathode Isolation Choke Joints

RF choke joint

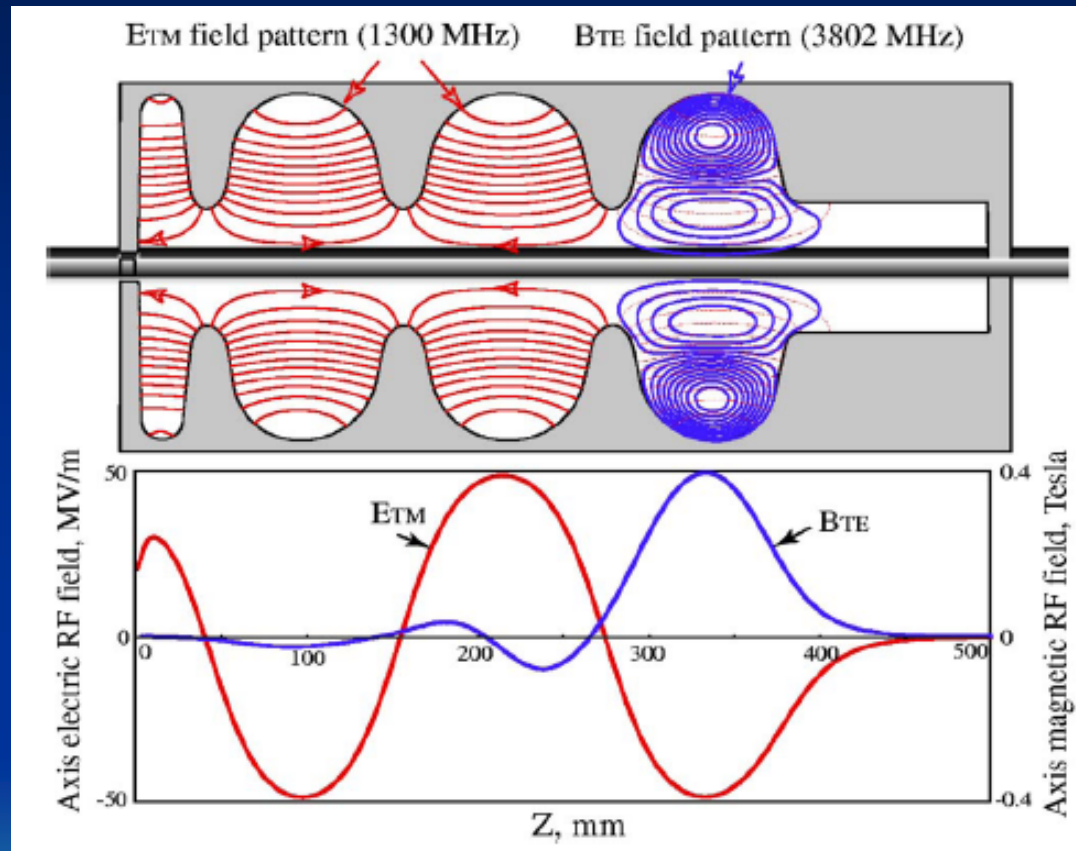


Quarter-wave choke joint



Two methods exist for electrically and thermally isolating the photocathode from the SRF cavity. Both methods involve setting up a standing wave null at the cathode to prevent RF from leaking out of the SRF cavity, hence the term choke joints or choke filters. The RF choke has been tested on the Rossendorf injector.

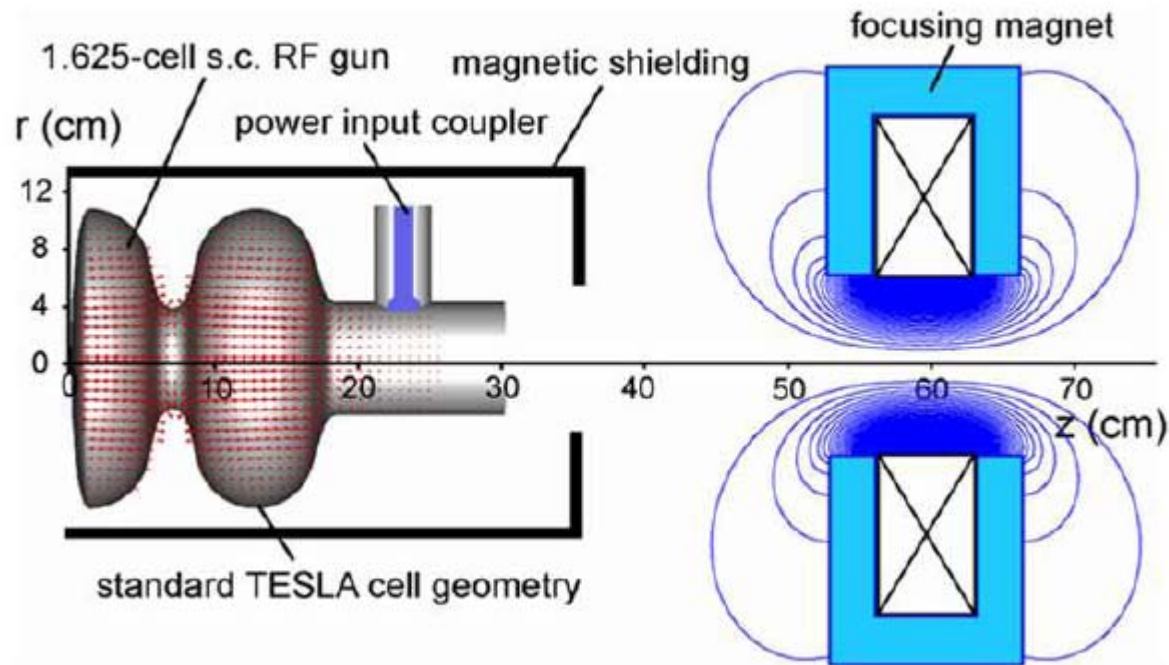
# Emittance Compensation with a Magnetic (Higher Order) Mode



Courtesy of  
J. Teichert

Magnetic higher order modes can be excited by the fundamental in an SRF cavity and provide axial magnetic field for performing emittance compensation.

# Emittance Compensation with an External Solenoid



A superconducting solenoid electromagnet can be placed inside the cryostat to provide the axial field for emittance compensation. The electromagnet must be turned on after the SRF cavity has been cooled to below the critical temperature.

# References

## Books and Article

RF Superconductivity

H. Padamsee

Handbook of Accelerator Physics and Engineering

Alex Chao

“RF and space charge effects in RF electron guns” K.J. Kim  
Nucl. Instr. Meth. Phys. A V. 275 (1989) 201-218

## URL

SRF07 Workshop

<http://web5.pku.edu.cn/srf2007/proceedings.html>

ICFA Newsletter

<http://www-bd.fnal.gov/icfabd/Newsletter46.pdf>

High-power Workshop

<http://home.physics.ucla.edu/power/indux.html>